



---

# *Journal of Statistical Software*

---

MMMMMM YYYY, Volume VV, Issue II. doi: 10.18637/jss.v000.i00

---

## **OpenFoam Assignment | The Mach 3 Step**

**Justin Campbell**

**Amanda Hiett**

**Akhil Sadam**

---

### **Abstract**

-SAMPLE ABSTRACT-

*Keywords:* computational fluid dynamics, CFD, incompressible, Paraview, R, Python, coe347, spring 2022.

---

### **1. Motivation**

The flow over a Mach 3 step is a well-studied problem in CFD (computational fluid dynamics), making it a good choice for convergence and performance studies. A simple set of studies are undertaken here.

### **2. Implementation**

We implement all simulation with OpenFoam, analysis with Paraview and Python3, and documentation code in R [Xie, Dervieux, and Riederer \(2020\)](#).

### **3. Theory : Governing Equations**

## Part 4: Governing Equations

## Problem Statement

The governing equations for this problem are the two-dimensional Euler equations, complemented with the equation of state for an ideal gas with  $\gamma = 1.4$ .

In your report:

- Write down the governing equations in vector form. Identify clearly the state vector  $\mathbf{U}$ , the  $x$  and  $y$  components of the flux ( $\mathbf{F}$  and  $\mathbf{G}$ , respectively), and any additional equation that relates the variables together, e.g. the equation of state.
- Include working definitions of the local Mach number of the flow and the local sound speed. You will need those definitions when plotting quantities.
- Apply basic normal shock and isentropic flow relations to estimate the pressure at the stagnation point on the surface of the step at  $(x, y) = (0.6, 0)$  for free stream conditions of  $M = 3$  and  $p = 1$  Pa.

## **Solutions**

## 4) Governing Equations

### Development of Governing Equations in Vector Form

Let us begin with the differential form of the momentum equation:

$$\frac{\partial \rho u}{\partial t} + \nabla \cdot (\rho u \otimes u) = -\nabla p + \nabla \cdot \tau + \rho b. \quad (1)$$

Given that the governing equations for the problem are the two-dimensional Euler equations, combined with the equation of state for an ideal gas with  $\gamma = 1.4$ , we can take the inviscid (Euler) flow limit of the equation neglecting viscous stresses and body forces.

$$\frac{\partial \rho u}{\partial t} + \nabla \cdot (\rho u \otimes u) = -\nabla p + \rho b + \rho f. \quad (2)$$

The differential form of the continuity equation can be expressed as

$$\frac{\partial \rho}{\partial t} + \nabla \cdot (\rho u) = 0 \quad (3)$$

The differential form of the energy equation can be expressed as

$$\frac{\partial \rho E}{\partial t} + \nabla \cdot (\rho E u) = \nabla \cdot (\lambda \nabla T) + \nabla \cdot (\sigma \cdot u) + s + \rho b \cdot u \quad (4)$$

Maintaining the equation by substituting for "σ" gives,

$$\frac{\partial \rho E}{\partial t} + \nabla \cdot (\rho E u) = \nabla \cdot (\lambda \nabla T) + \nabla \cdot (\tau \cdot u) + s + \rho b \cdot u \quad (5)$$

Taking the inviscid (Euler) flow limit of the equation neglecting viscous stresses and assuming that there are no body forces or heat addition in the flow,  $b=0$ ,  $Q=s+\rho b \cdot u=0$ , and  $\nabla T=0$ , and  $\tau=0$  gives

$$\frac{\partial \rho E}{\partial t} + \nabla \cdot (\rho E u) = 0 \quad \text{or} \quad s = 0 \quad (6)$$

$$\text{Here, } H = E + \frac{P}{\rho} = h + \frac{u^2}{2} \quad (7)$$

Let us return to the momentum equation (2) and expand the LHS of the expression giving,

$$\frac{\partial \rho u}{\partial t} + \nabla \cdot (\rho u \otimes u) = \rho \left\{ \frac{\partial u}{\partial t} + u \cdot \nabla u \right\} + u \left\{ \frac{\partial \rho}{\partial t} + \nabla \cdot (\rho u) \right\} \quad \begin{matrix} \text{(from continuity)} \\ \cancel{\text{Equation (3)}} \end{matrix}$$

$$\Rightarrow \frac{\partial \rho u}{\partial t} + \nabla \cdot (\rho u \otimes u) = \rho \left\{ \frac{\partial u}{\partial t} + u \cdot \nabla u \right\} \quad (8)$$

Substituting the RHS of equation (8) into the LHS of equation (2) gives

$$\rho \left\{ \frac{\partial u}{\partial t} + u \cdot \nabla u \right\} = -\nabla p \quad (9)$$

w  
local acceleration    convective acceleration

But,  $\frac{\partial u}{\partial t} + u \cdot \nabla u = \frac{D u}{D t}$  giving,

$$\rho \frac{D u}{D t} = -\nabla p \quad (10)$$

Dividing equation (10) by " $\rho$ " gives

$$\frac{D u}{D t} = -\frac{\nabla p}{\rho}$$

Then, since the rescaled (normalized) pressure,  $\pi = \frac{p}{\rho}$ , we have,

$$\frac{D u}{D t} = -\nabla \pi \quad (11)$$

Separating equation (11) using the identities for the total acceleration and rescaled pressure according to  $x$  and  $y$  components gives,

$$x: \frac{\partial u}{\partial t} + u \frac{\partial u}{\partial x} + v \frac{\partial u}{\partial y} = -\frac{2(\frac{p}{\rho})}{2x} \quad (12)$$

$$y: \frac{\partial v}{\partial t} + u \frac{\partial v}{\partial x} + v \frac{\partial v}{\partial y} = -\frac{2(\frac{p}{\rho})}{2y} \quad (13)$$

Let us now return to the Continuity Equation (3) and expand the LHS of the expression given,

$$\frac{\partial \rho}{\partial t} + \left[ \left( \frac{\partial}{\partial x}, \frac{\partial}{\partial y} \right) \cdot (\rho u, \rho v) \right] = 0$$

$$\frac{\partial \rho}{\partial t} + \frac{\partial \rho u}{\partial x} + \frac{\partial \rho v}{\partial y} = 0 \quad (14)$$

Lastly, let us return to the Energy equation (6) and expand the LHS of the expression given,

$$\frac{\partial \rho E}{\partial t} + \nabla \cdot (\rho H u) = 0 \quad (\text{where } H = E + \frac{P}{\rho})$$

$$\Rightarrow \frac{\partial \rho E}{\partial t} + \nabla \cdot \left( \rho \left( E + \frac{P}{\rho} \right) u \right) = 0$$

$$\Rightarrow \frac{\partial \rho E}{\partial t} + \nabla \cdot (\rho E u + \rho u) = 0$$

$$\Rightarrow \frac{\partial \rho E}{\partial t} + \left( \frac{\partial}{\partial x}, \frac{\partial}{\partial y} \right) \cdot \left( \rho E \begin{bmatrix} u \\ v \end{bmatrix} + \rho \begin{bmatrix} u \\ v \end{bmatrix} \right) = 0$$

$$\Rightarrow \frac{\partial \rho E}{\partial t} + \left( \frac{\partial}{\partial x}, \frac{\partial}{\partial y} \right) \cdot (\rho E u + \rho u, \rho E v + \rho v) = 0$$

$$\Rightarrow \frac{\partial \rho E}{\partial t} + \frac{\partial}{\partial x} (\rho E u + \rho u) + \frac{\partial}{\partial y} (\rho E v + \rho v) = 0 \quad (15)$$

Now, the governing equations can be expressed in vector form with a single vector equation that can be interpreted as a conservation equation for the far field. Simplified N=5 equations broken down into a vector with time-dependent terms, and two vectors with space-dependent terms as,

$$\frac{\partial \mathbf{U}}{\partial t} + \frac{\partial \mathbf{F}}{\partial x} + \frac{\partial \mathbf{G}}{\partial y} = 0 \quad (16)$$

(where  $\mathbf{U}$  is the state vector,  $\mathbf{F}$  is the  $x$ -constant of the flux  ~~$\mathbf{F}$~~ , and  $\mathbf{G}$  is the  $y$ -component of the flux).

The state vector, "U" contains the time gradient terms from each of the four variables.

Continuity:  $\rho$

X-momentum:  $\rho u$

y-momentum:  $\rho v$

Energy:  $\rho e$

$$\Rightarrow U = \begin{bmatrix} \rho \\ \rho u \\ \rho v \\ \rho e \end{bmatrix}$$

the flux vector, "F", contains the X-gradient terms,

Continuity:  $\rho u$

X-momentum:  $\rho u^2 + p$

y-momentum:  $\rho uv + p$

Energy:  $\rho ut + pe$

$$F(u) = \begin{bmatrix} \rho u \\ \rho u^2 + p \\ \rho uv + p \\ \rho ut + pe \end{bmatrix}$$

the flux vector, "G", contains the y-gradient terms,

Continuity:  $\rho v$

X-momentum:  $\rho uv + p$

y-momentum:  $\rho v^2 + p$

Energy:  $\rho vt + pe$

$$G(v) = \begin{bmatrix} \rho v \\ \rho uv + p \\ \rho v^2 + p \\ \rho vt + pe \end{bmatrix}$$

The Equation of State for an ideal, calorically perfect gas is expressed as,

$$\underline{PRT = P} \quad (17)$$

(where "R" is the gas constant in  $\text{J kg}^{-1}\text{K}^{-1}$ , "T" is the temperature in K, and "P" is the pressure in  $\text{N m}^{-2}$ ).

The gas constant is expressed as,

$$\underline{R = \frac{R}{w}} \quad (18)$$

(where "R" is the universal gas constant,  $\text{J mol}^{-1}\text{K}^{-1}$ , and "w" is the molar mass of the gas in  $\text{kg mol}^{-1}$ ).

The universal gas constant, "R" equals,

$$R = 8314 \text{ J mol}^{-1}\text{K}^{-1}$$

Again, for an ideal, calorically perfect gas,

$$\underline{e = \frac{P}{\rho} \frac{1}{\gamma-1} = \frac{R}{\gamma-1} T = C_p T} \quad (19)$$

where  $\gamma = \frac{C_p}{C_v}$ ,  $C_p = \frac{R}{\gamma-1}$ , and  $C_v = C_p - R$

The Speed of sound can be expressed as:

$$\underline{a = \sqrt{\gamma RT} = \sqrt{\frac{\gamma P}{\rho}}} \quad (20)$$

Now, we can recover pressure from the state vector by rearranging equation (19)

$$\underline{P = (\gamma-1)Pe = (\gamma-1)(E - \rho U^2/2)} \quad (21)$$

The local mach Number of the flow is quantified according to:

$$\boxed{\underline{Ma = \frac{|U|}{a}}} \rightarrow \begin{array}{l} \text{(magnitude of local velocity)} \\ \text{local sound speed} \end{array} \quad (22)$$

Estimation of pressure at stagnation point on surface of step at  $(x, y) = (0.6, 0)$

Given free-stream conditions,  $Ma = 3$ ,  $P = 1$ ,  $\gamma = 1.4$   
and that density equals

$$\rho = \frac{\gamma P}{a^2} = \gamma = 1.4$$

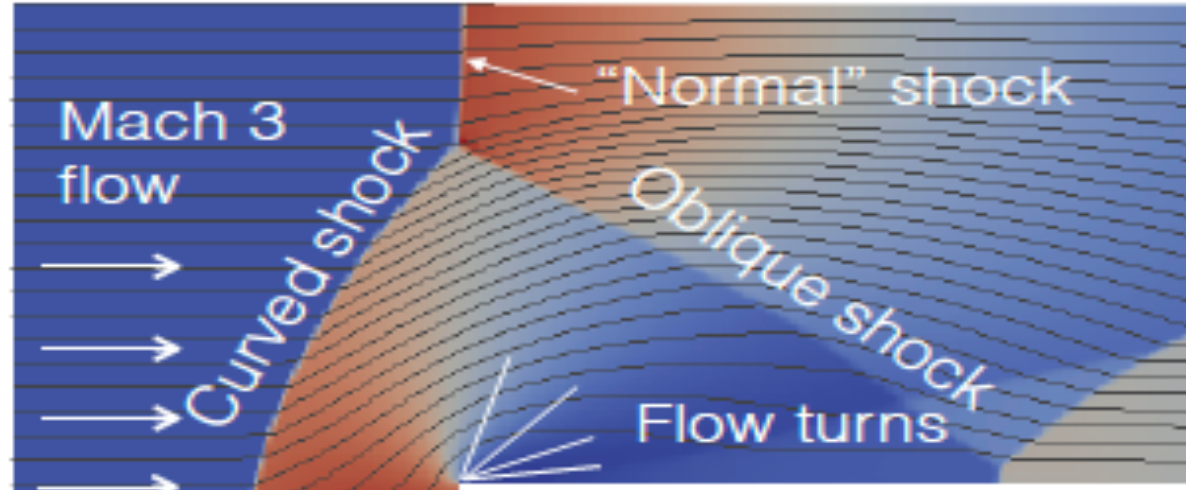
Equation (20) can be used to obtain the speed of sound

$$a = \sqrt{\frac{\gamma P}{\rho}} = \sqrt{\frac{(1.4)(1 \text{ Pa})}{1.4 \text{ kg/m}^3}} = 1 \text{ m/s}$$

Substitution of  $a = 1 \text{ m/s}$  and  $Ma = 3$  into equation (20) gives  
the magnitude of local velocity in the free-stream,

$$|U| = Ma \cdot a = (3)(1 \text{ m/s}) = 3 \text{ m/s}$$

In referencing the flow streamlines over the computational grid in the slide "Flow Streamlines" in lecture16.pdf, it is shown that expected behavior contains a shock wave generated normal to the streamlines between the free stream and the stagnation point over  $(x, y) = (0, 0)$  to  $(x, y) = (0.6, 0)$ . This region is highlighted in the figure below.



Free Stream  
Point with  $P = 1$   
 $P_a, Ma = 3$

1      2      3

**Stagnation point**

**Leading shock**

Point Downstream  
of Normal Shock  
Wave

According to NASA documentation on Normal Shock wave properties in compressible flow, "For compressible flows with little or small flow turning, the flow process is reversible and the entropy is constant, the change in flow properties are then given by the isentropic relations. The region in the freestream that is compressible flow with little flow turning is then compatible with this definition. The documentation then proceeds to state the following regarding Shock waves, "If the shock wave is perpendicular to the flow direction it is called normal shock." Again, referencing the illustration above, it can be assumed for simplicity that the behavior of the flow at the streamlines intersecting the bottom of the curved shock field and the stagnation point exhibits normal shock since the streamline is normal to the shock region along this line. Operating off of this assumption, equations 23) and 24) below are used describe the change in flow properties across a normal shock wave :

$$M_{a2}^2 = \frac{(\gamma - 1) M_{a1}^2 + 2}{2 \gamma M_{a1}^2 - (\gamma - 1)} \quad (23)$$

(where "M<sub>a2</sub>" is the Mach Number to the right of the Normal shock wave  
 "M<sub>a1</sub>" is the Mach Number of the free stream)  
 (downstream)

$$\frac{P_2}{P_1} = \frac{2\gamma M_{a1}^2 - (\gamma - 1)}{\gamma + 1} \quad (24)$$

(where "P<sub>2</sub>" is the Static pressure downstream Normal shock wave region, "P<sub>1</sub>" is the static pressure in the freestream).

Substitution of  $\gamma = 1.4$ ,  $M_{\infty} = 3$  into equation (23) and solving for "M<sub>2</sub>" gives,

$$M_{2} = \sqrt{\frac{(1.4-1)(3)^2 + 2}{2(1.4)(3)^2 - (1.4-1)}} \approx 0.4752$$

Rearranging equation (24) and solving for the static pressures,

$$\begin{aligned} P_2 &= P_1 \left( \frac{2\gamma M_{\infty}^2 - (\gamma-1)}{\gamma+1} \right) \\ &= (1 \text{ Pa}) \left( \frac{2(1.4)(5^2) - (1.4-1)}{1.4+1} \right) \\ &\approx 10.3333 \text{ Pa} \end{aligned}$$

Now, the region of the streamline between points 2 (downstream of shock wave) and 3 (stagnation point) is isentropic, meaning that the change in flow variables is small and gradual. In referencing NASA's article on "Isentropic flow" whose citation is provided at the end of the report, equation 25) below depicts the ratio of pressure change between two points in an isentropic flow region,

$$\frac{P_2}{P_t} = \left( 1 + \frac{\gamma-1}{2} M_{2}^2 \right)^{-\frac{\gamma}{\gamma-1}} \quad (25)$$

where " $P_2^{ll}$ " is the static pressure downstream in isentropic flow and " $P_t$ " is the total pressure at isentropic flow region (and at stagnation point).

Rearranging the equation to solve for the stagnation pressure gives,

$$\frac{P_2}{P_3} = \left( 1 + \frac{\gamma-1}{2} M_{2}^2 \right)^{-\frac{\gamma}{\gamma-1}}$$

$$P_3 = \left[ \left( 1 + \frac{\gamma-1}{2} M_{2}^2 \right)^{-\frac{\gamma}{\gamma-1}} \right] P_2 \approx \left[ \left( 1 + \frac{1.4-1}{2} (0.4752)^2 \right)^{\frac{1.4-1}{1.4-1}} \right] (10.333 \text{ Pa}) \approx 12.06 \text{ Pa}$$

(total)  
Therefore, the pressure at the stagnation point on the surface of the  
step at  $(x, y) = (0.6, 0)$  for free stream conditions of  $M = 3$   
and  $P = 1$  Pa is approximately 12.06 Pa.

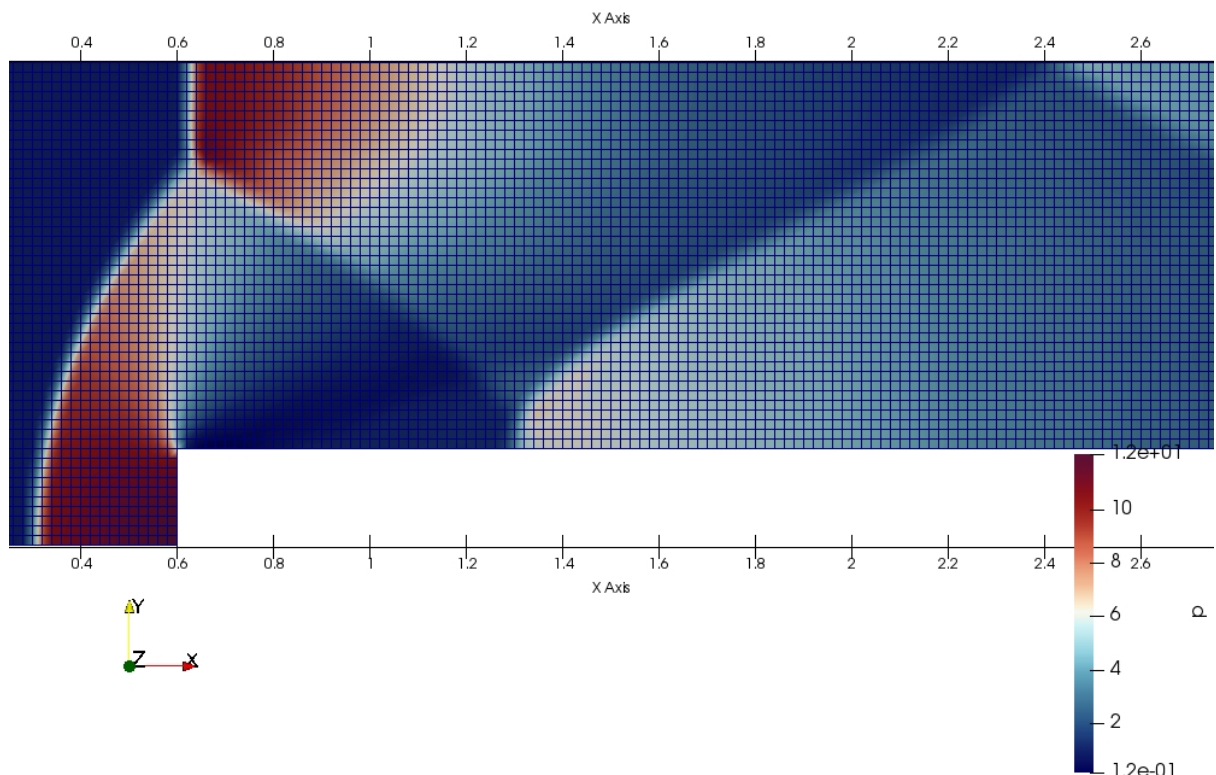
## References

- 1) "Normal Shock Wave Equations." Edited by Nancy Editor, *NASA*, NASA,  
<https://www.grc.nasa.gov/WWW/k-12/airplane/normal.html>.
- 2) "Isentropic Flow Equations." Edited by Nancy Hall, *NASA*, NASA,  
<https://www.grc.nasa.gov/WWW/K-12/airplane/isentrop.html>.

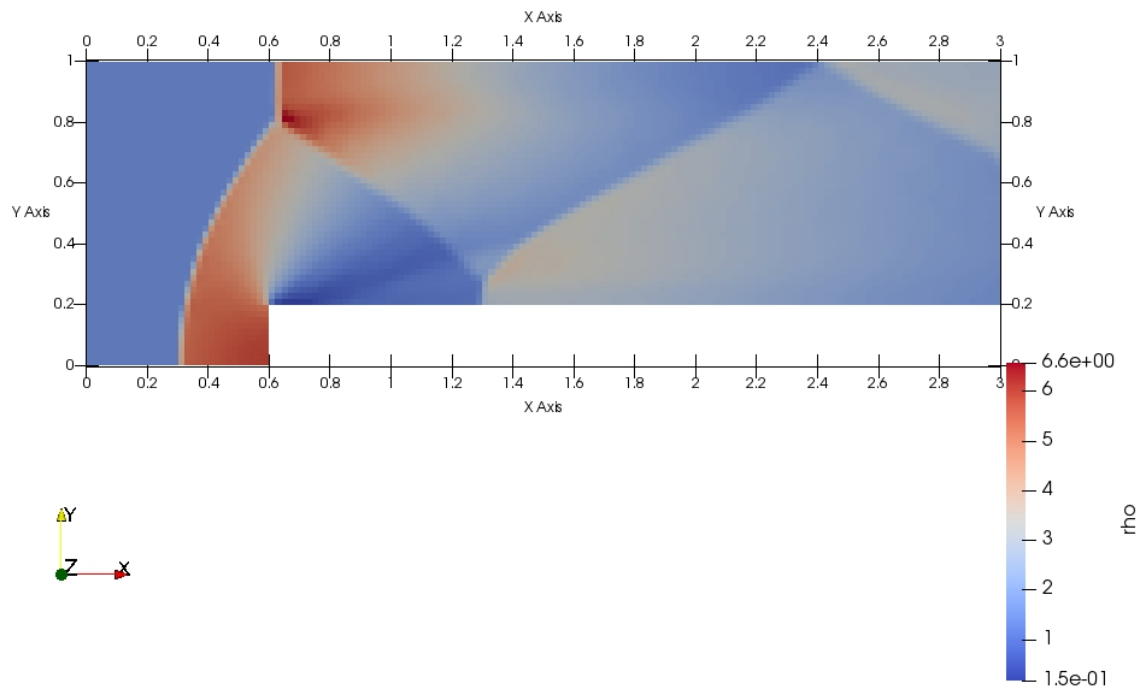
## 4. Mesh Assembly : Preliminaries

We assemble a preliminary solution at  $T = 4s$  with 6300 cells, for the following inlet conditions:  $M = 3, p = 1Pa, T = 1K, \rho = \gamma \frac{kg}{m^3}$  with  $\gamma = 1.4$ . All results have been non-dimensionalized: velocity, pressure, density and temperature are all measured with respect to inlet conditions.

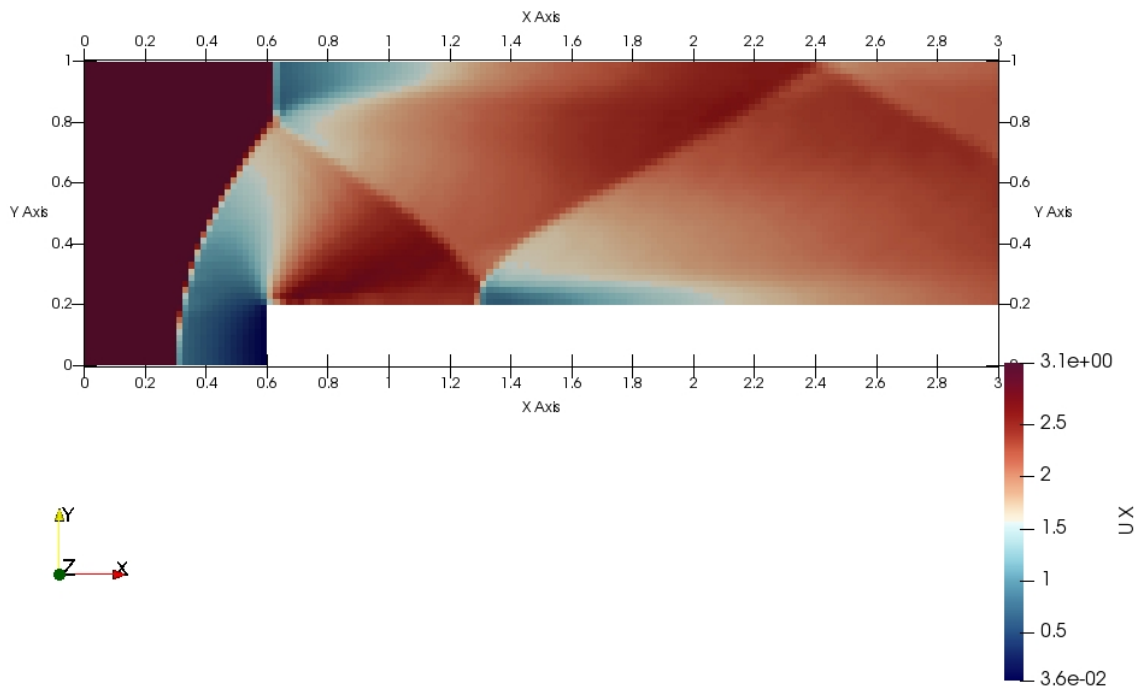
### 4.1. Mesh

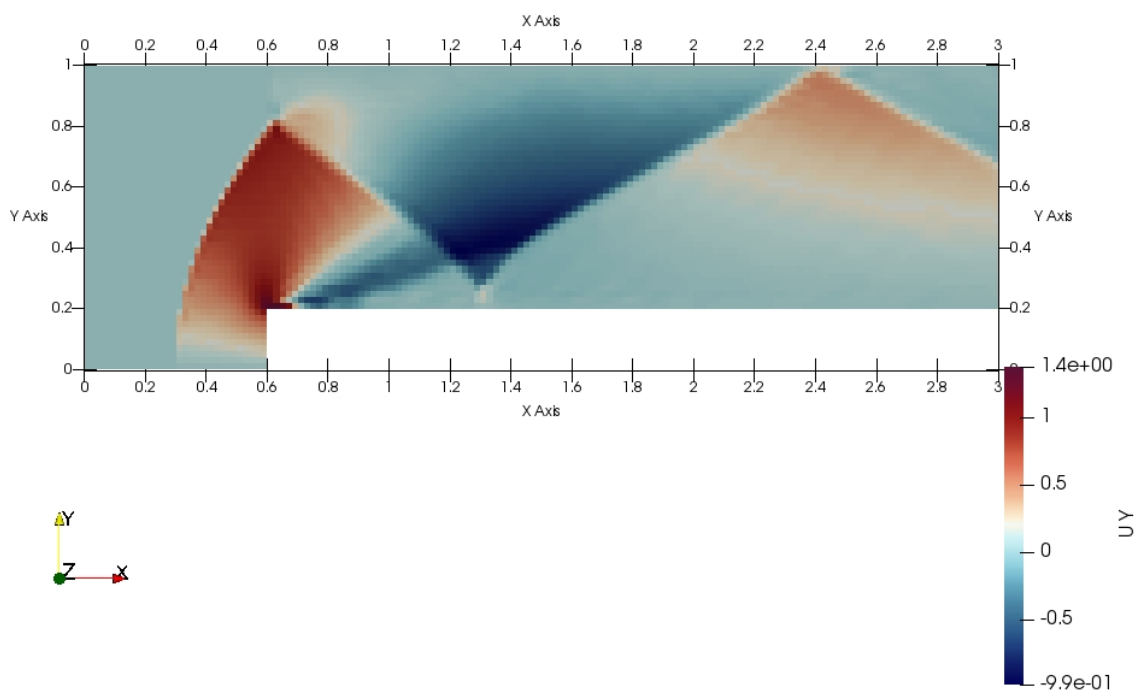


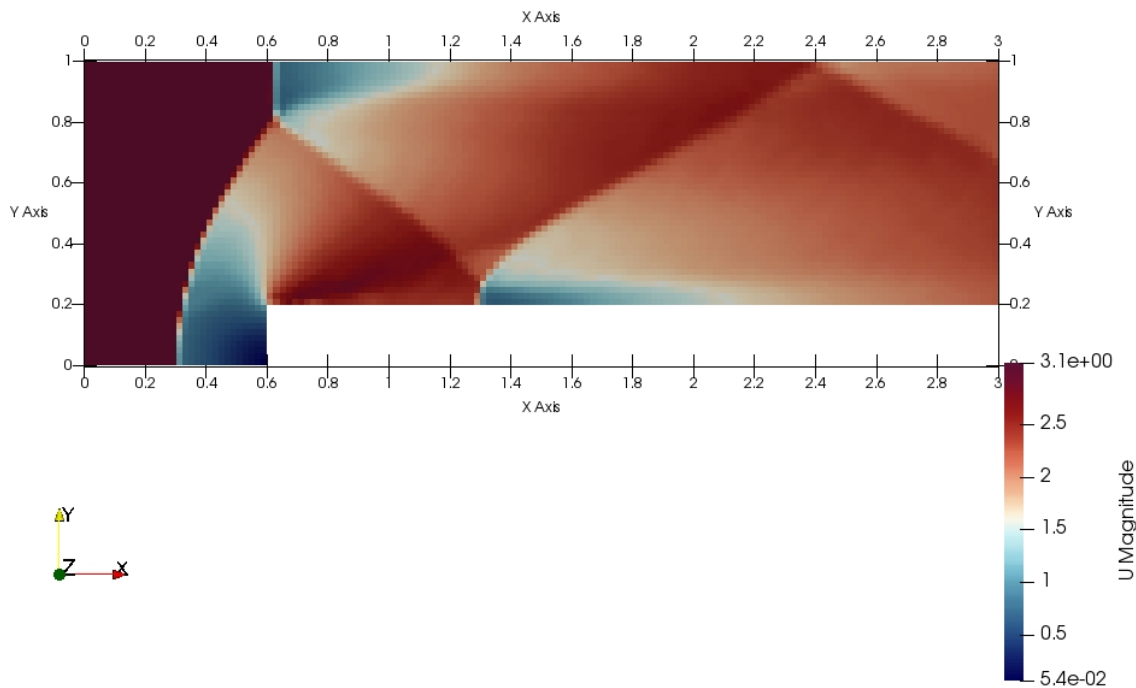
### 4.2. Density



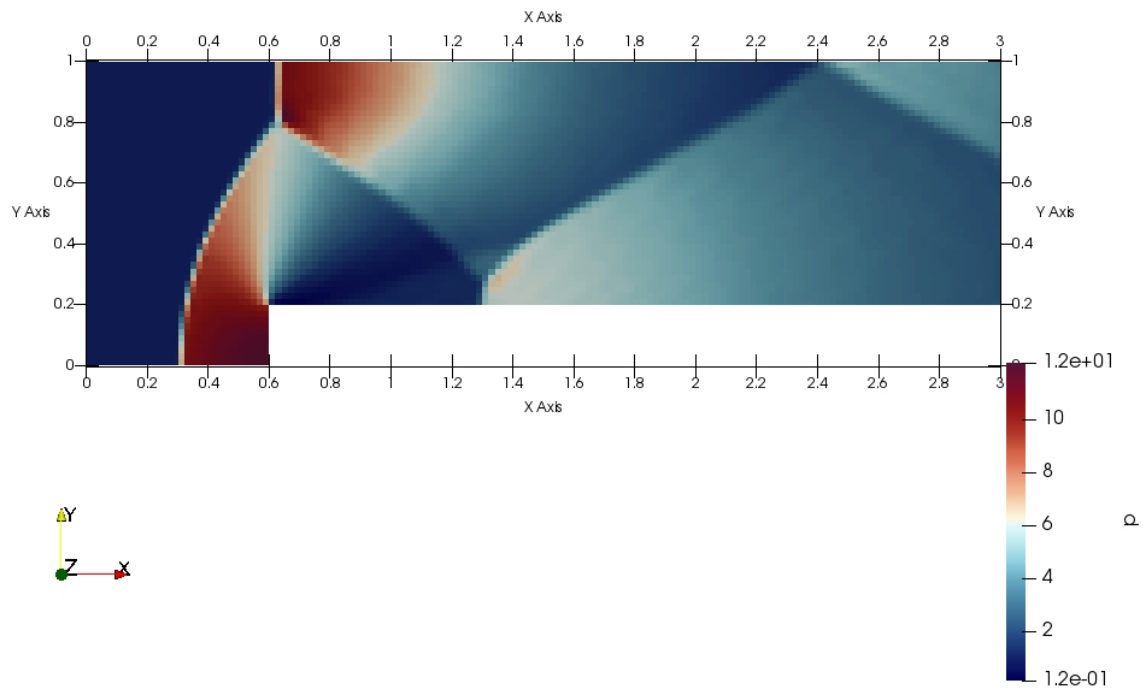
#### 4.3. Velocity X, Y, Magnitude



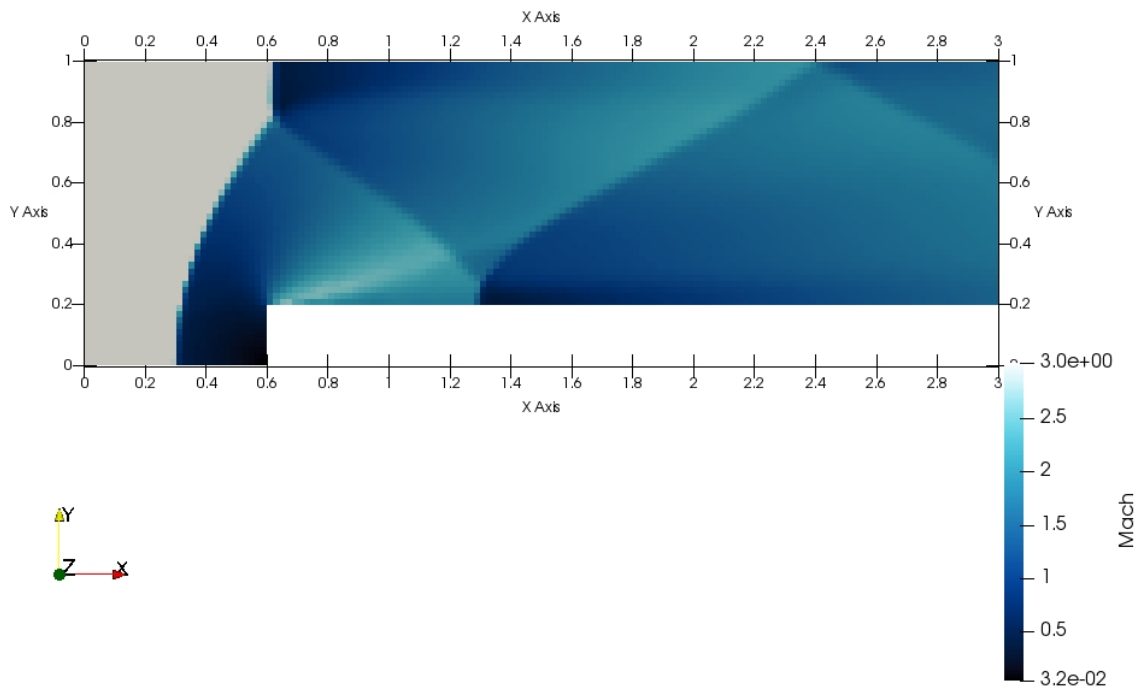




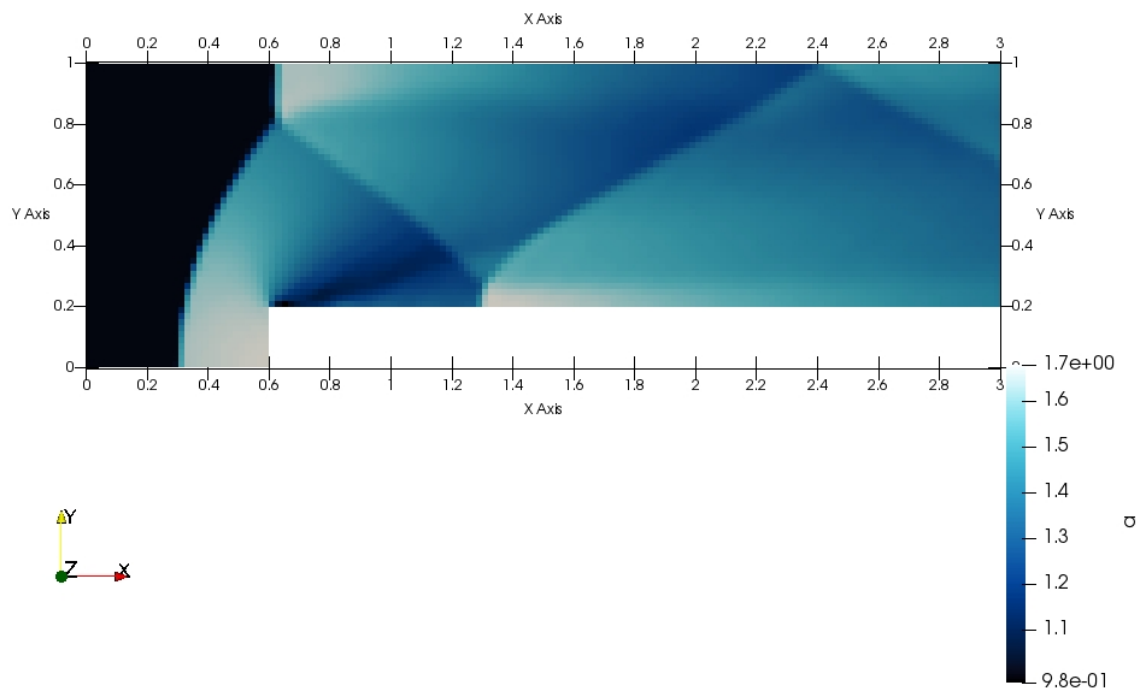
#### 4.4. Pressure



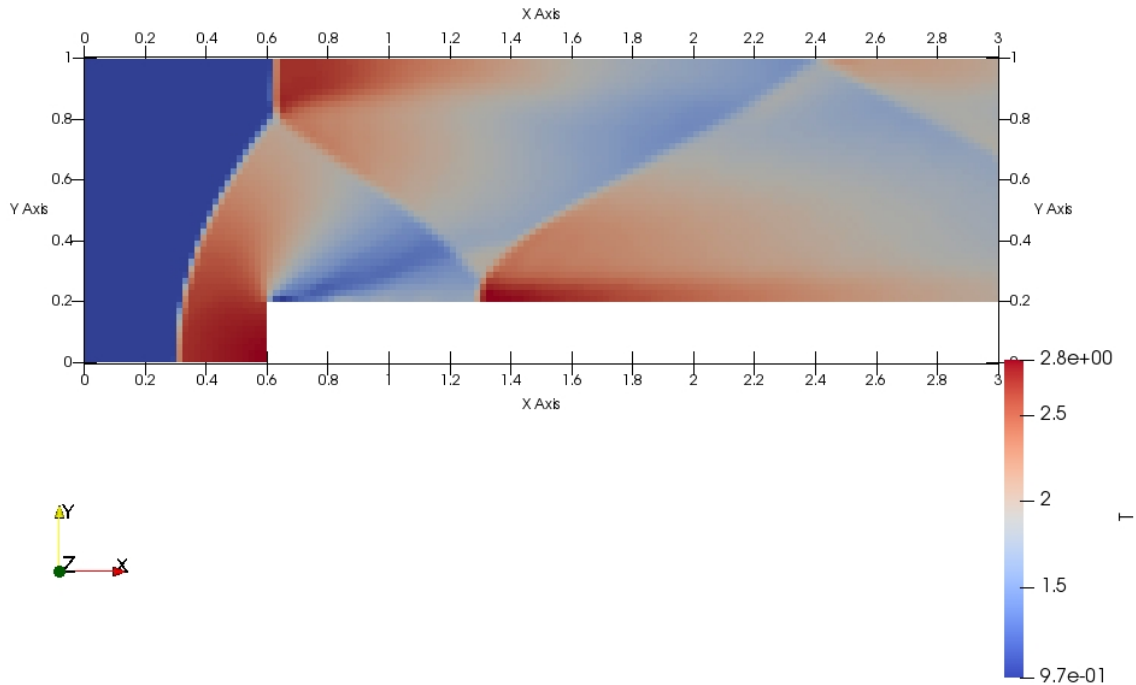
#### 4.5. Mach Number



#### 4.6. Speed of Sound



#### 4.7. Temperature



## 5. Convergence

Three meshes were used, with increasing numbers of cells and smaller timesteps, as follows: (note the timesteps are approximate as the solver, RhoCentralFoam, adjusts timesteps as necessary to maintain a maximum Courant number of 0.2).

Run\_10\_64 : 6300 cells,  $dx = 0.04000$ ,  $dt = 0.00110$

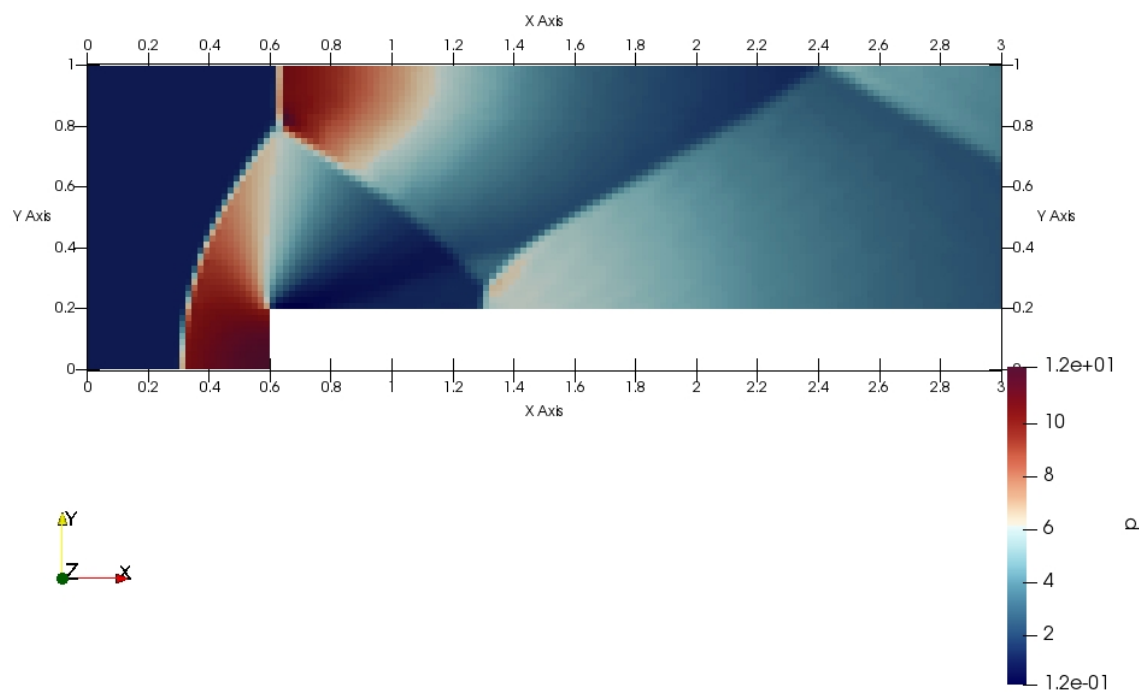
Run\_20\_64 : 25200 cells,  $dx = 0.02000$ ,  $dt = 0.00056$

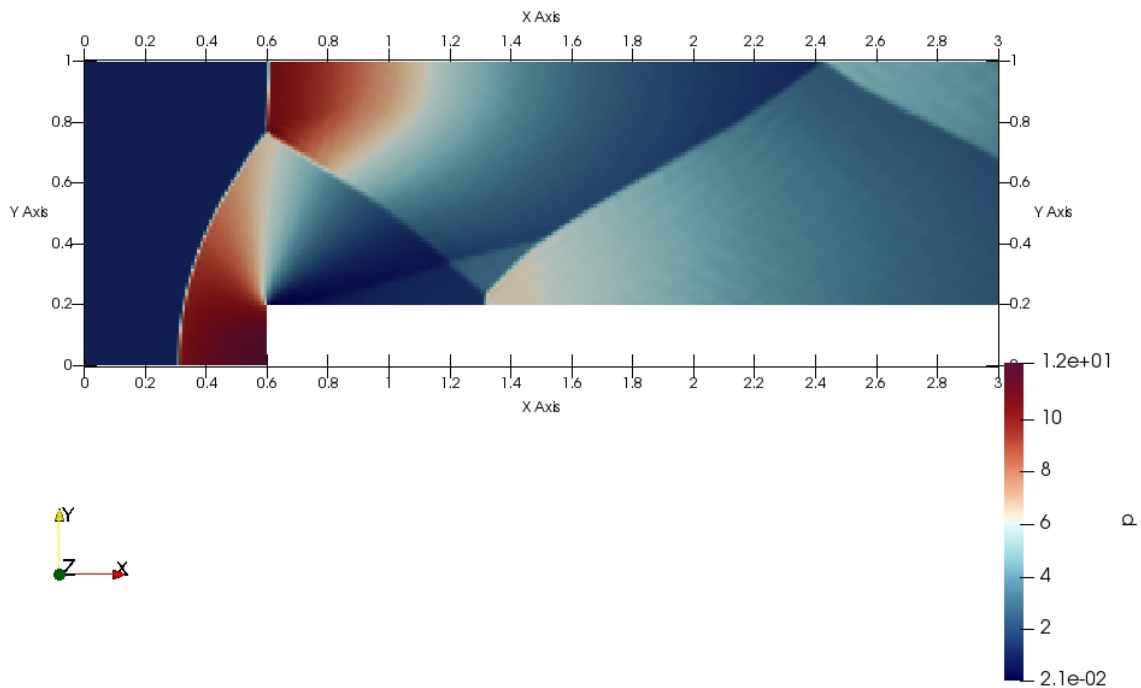
Run\_32\_64 : 64512 cells,  $dx = 0.00625$ ,  $dt = 0.00034$

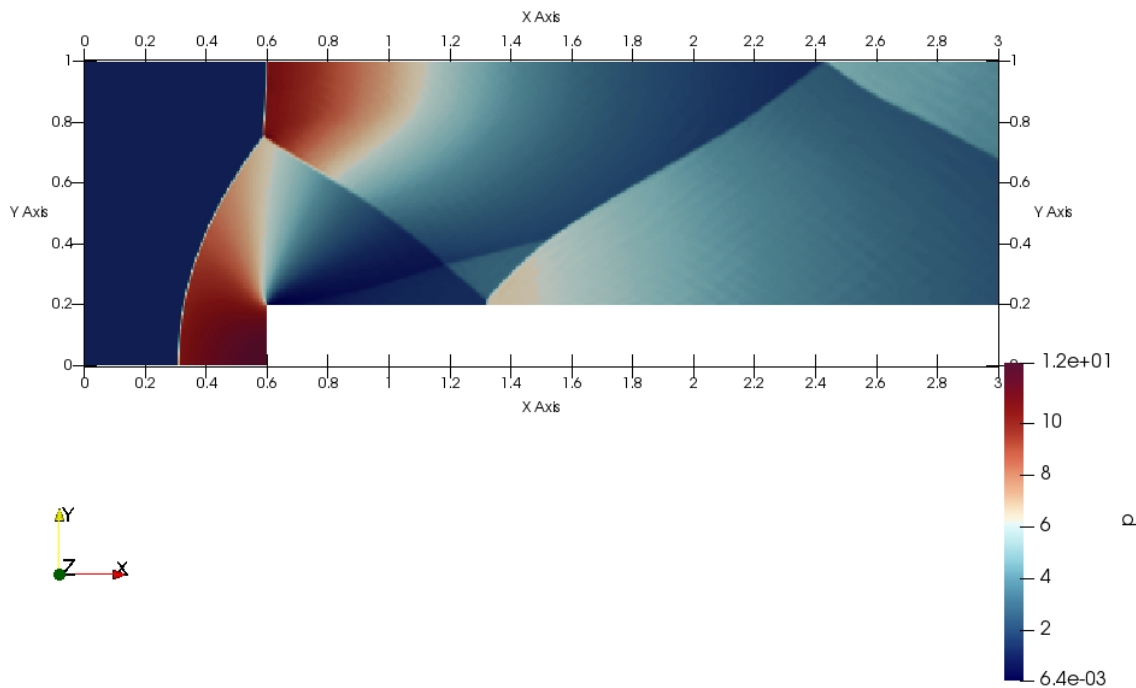
### 5.8. Improvements in Pressure, Density, and Y-Velocity with increasing resolution:

Note the upper shock turbulent features (the small waves), and how they resolve much more appropriately with higher resolution meshes.

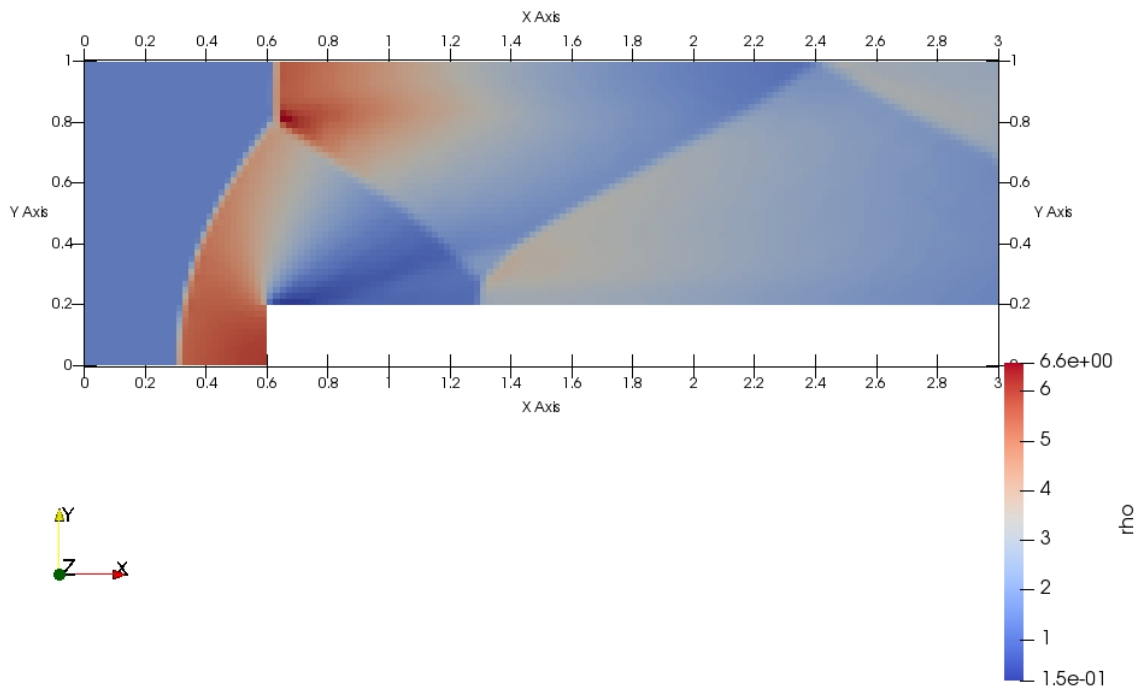
**Pressure (from Run\_10 to Run\_32):**

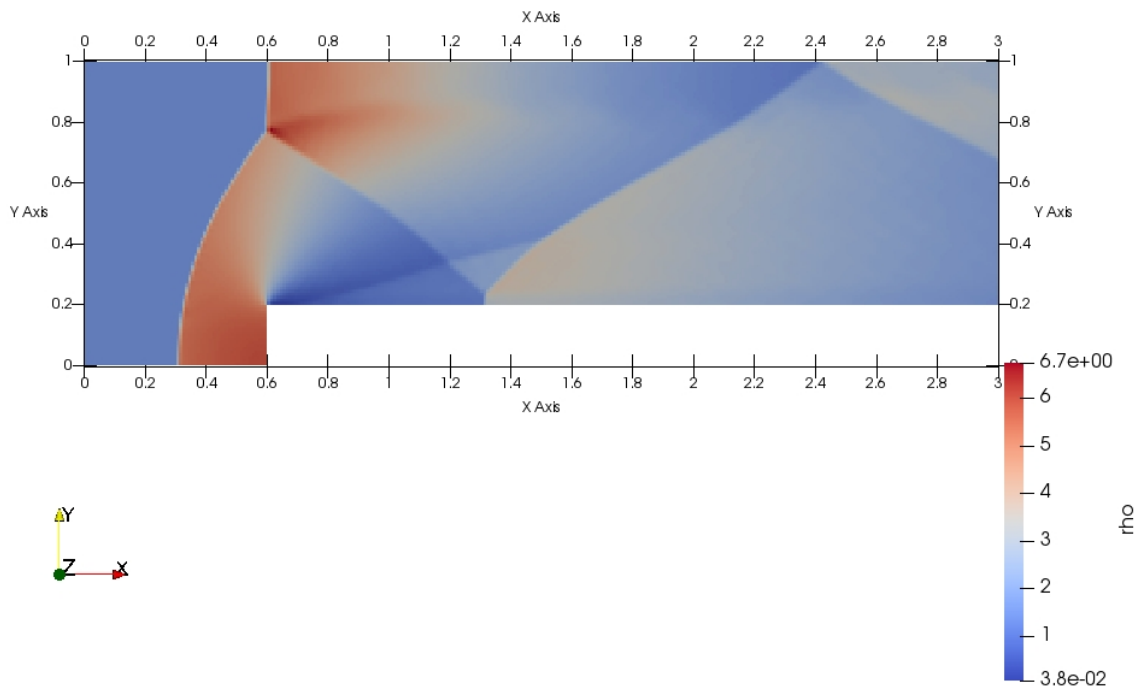


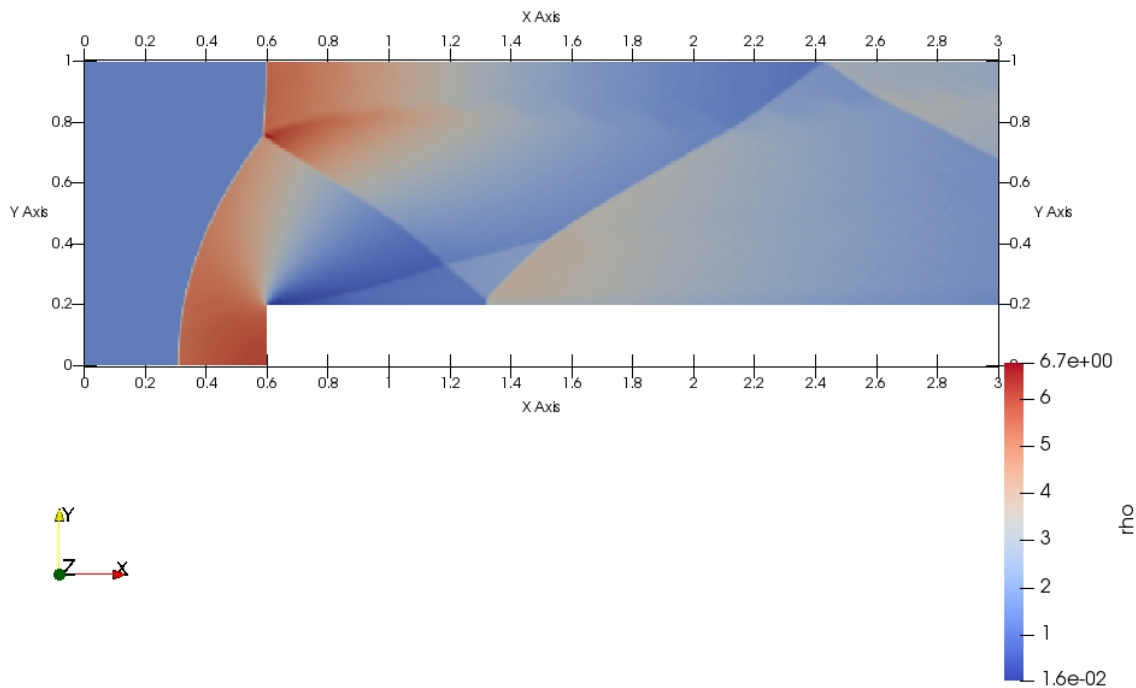




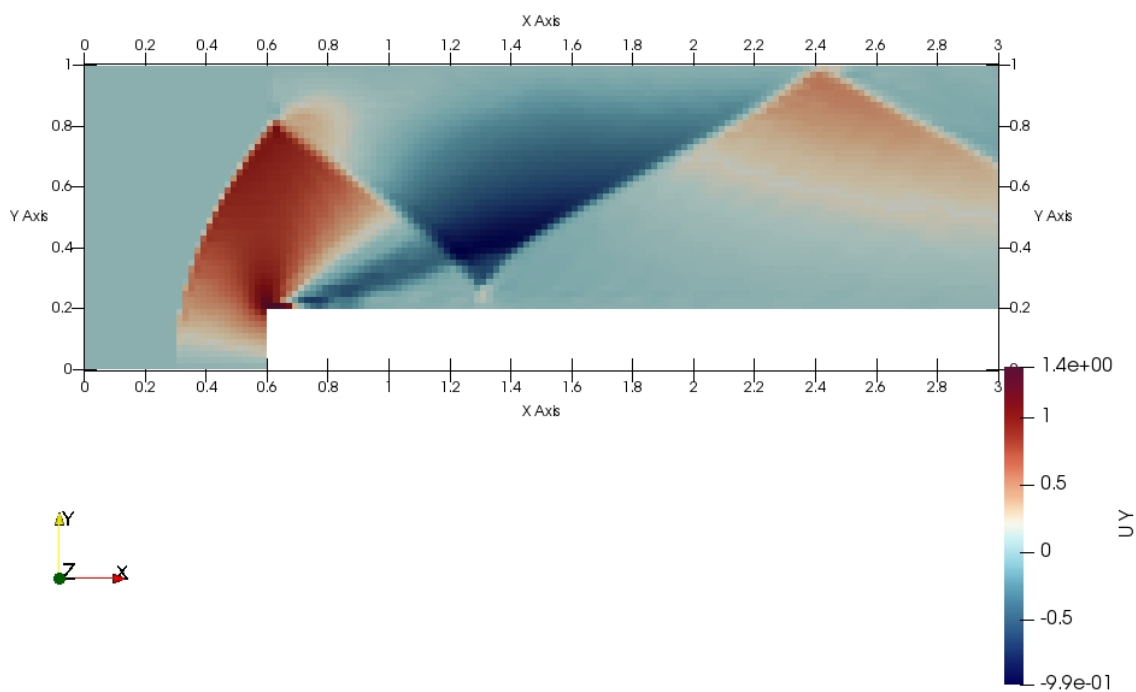
**Density:**

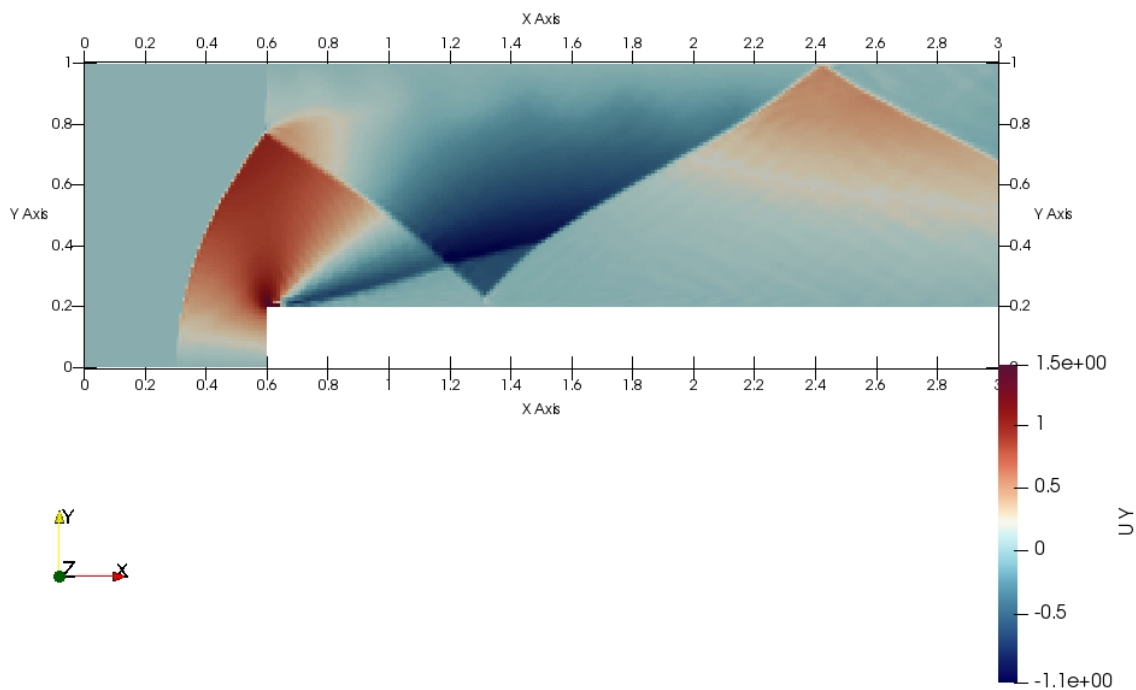


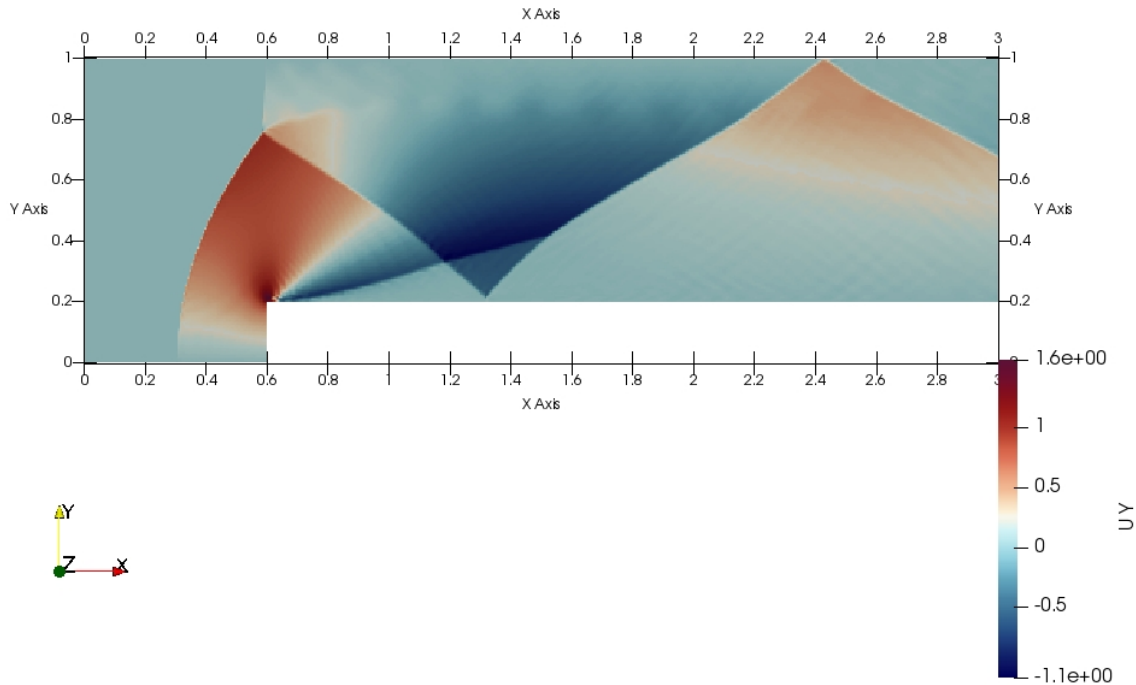




**Y-velocity:**



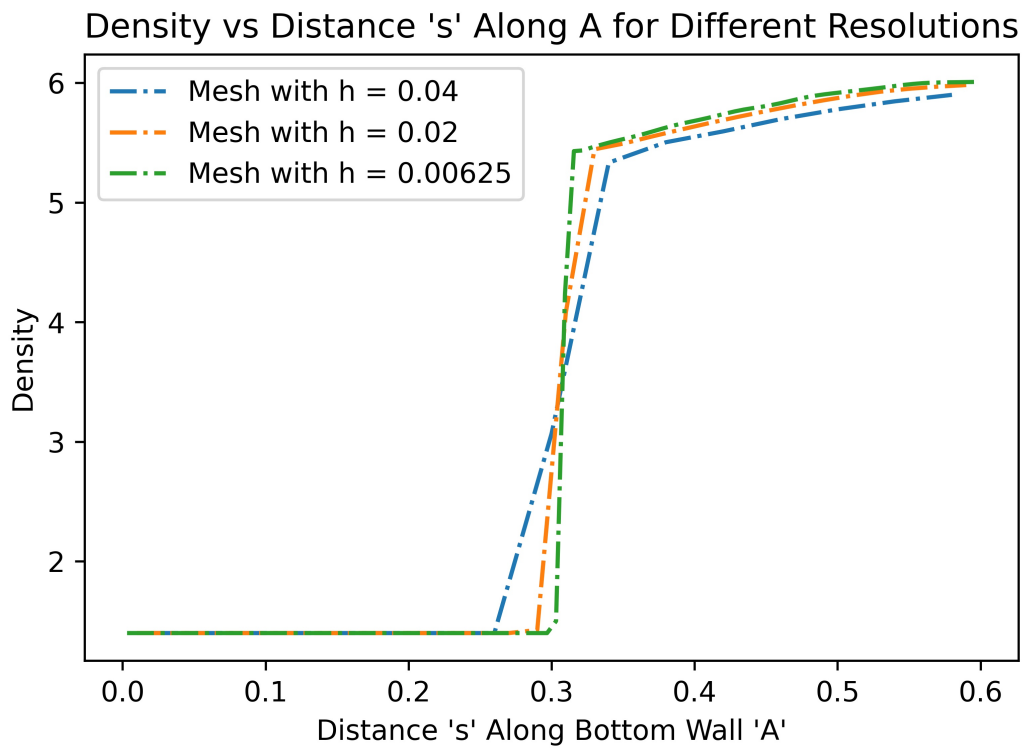
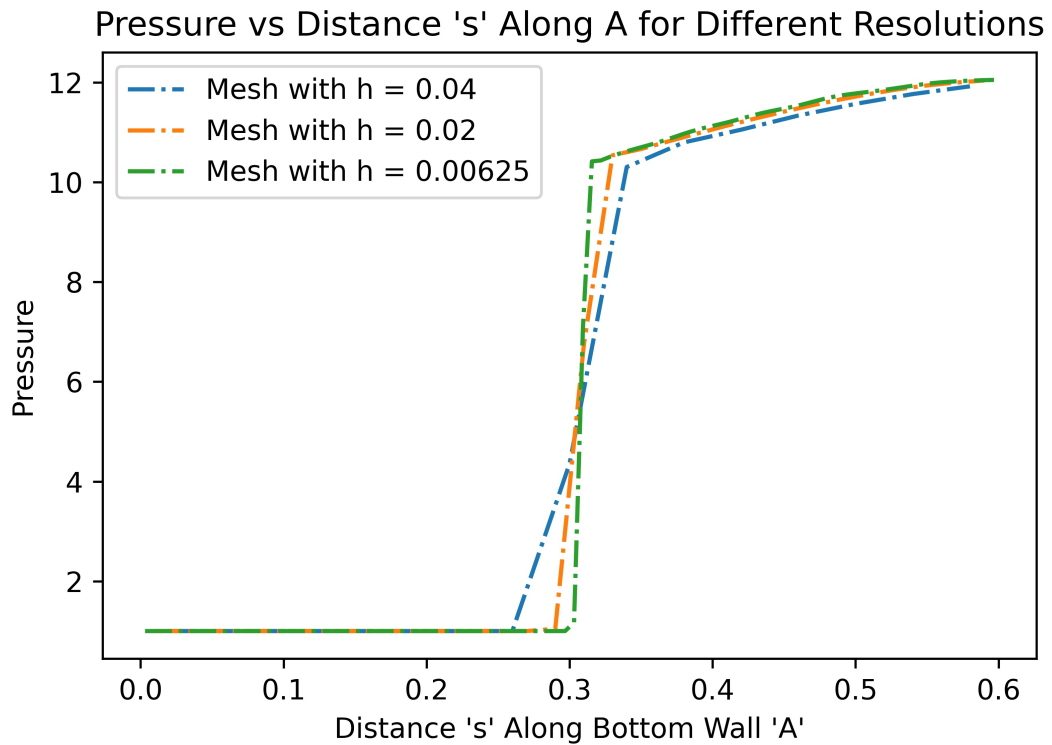


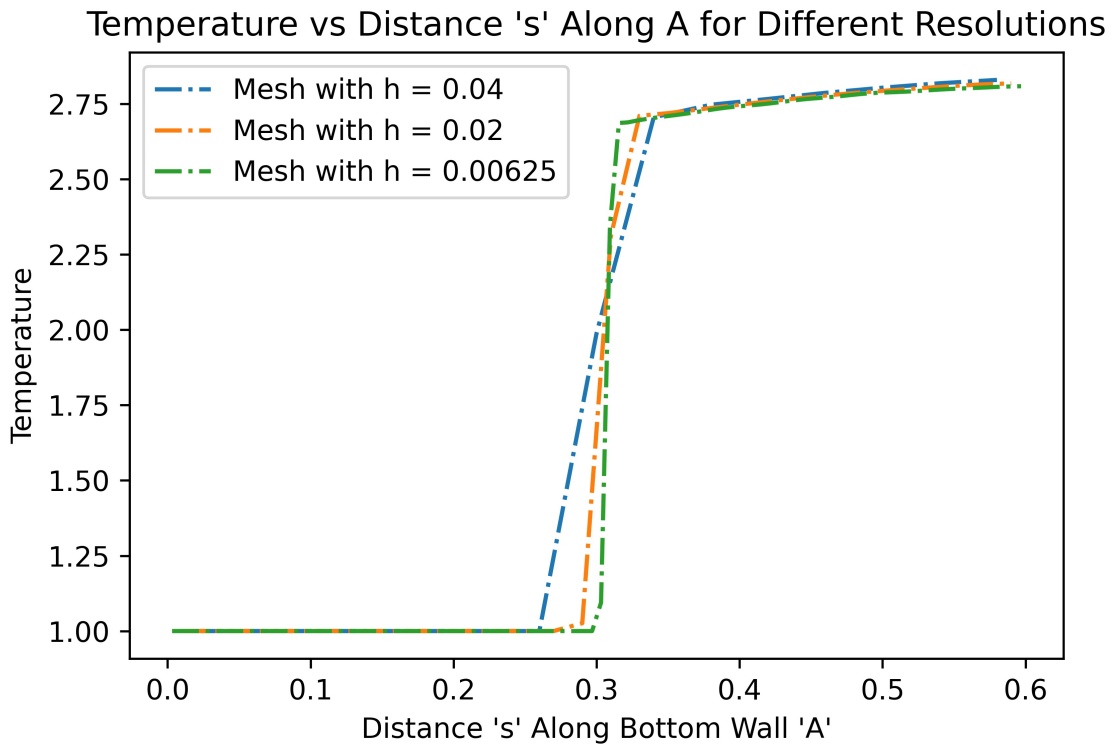


### 5.9. Wall Distributions w.r.t Resolution Levels:

To examine the convergence of solution fields with a refinement of the mesh and associated reduction in grid spacing, plots of the pressure, temperature, fluid density, and x and y components of velocity were developed against the distance along four surfaces of interest, namely, the bottom wall, “A”, the vertical step wall, “B”, the bottom step wall, “C”, and the top wall, “D”. The purpose of generating these plots was to observe the underlying patterns, and convergence of these solution fields to theoretical behavior.

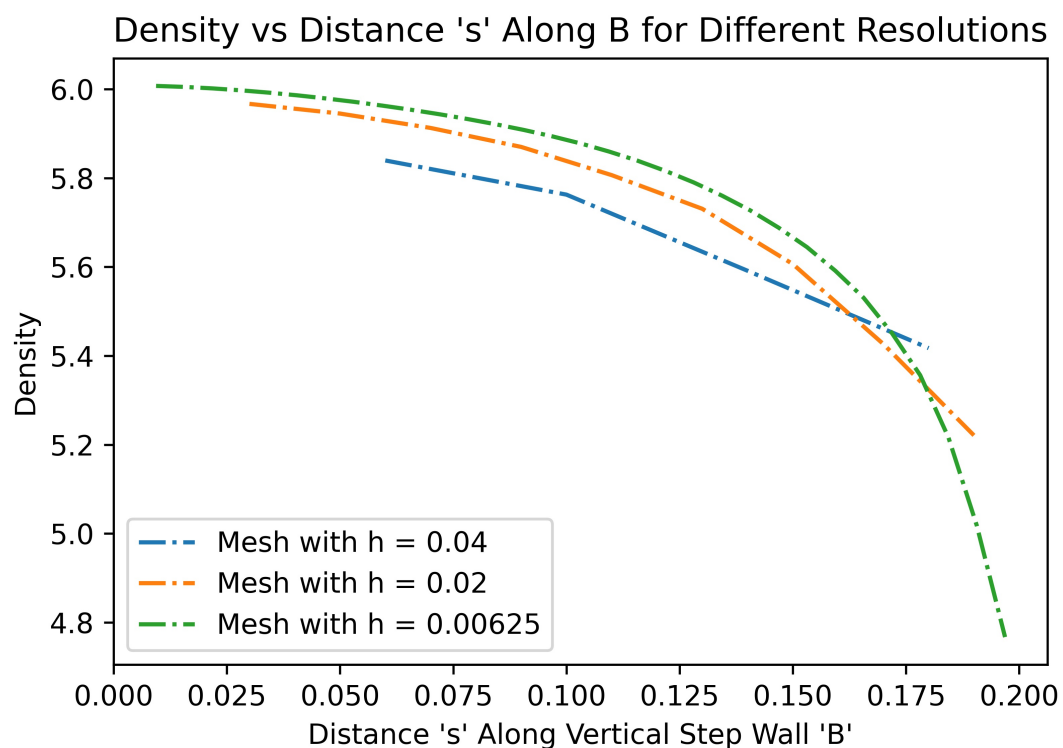
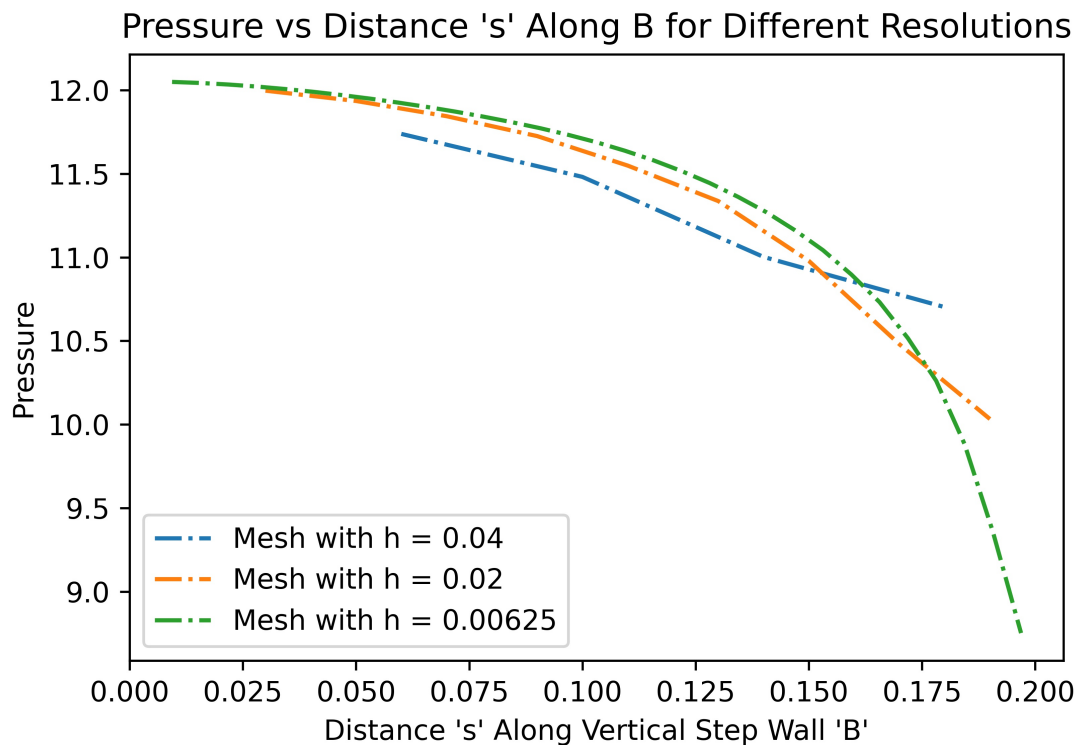
#### Wall A Pressure, Density, Temperature:

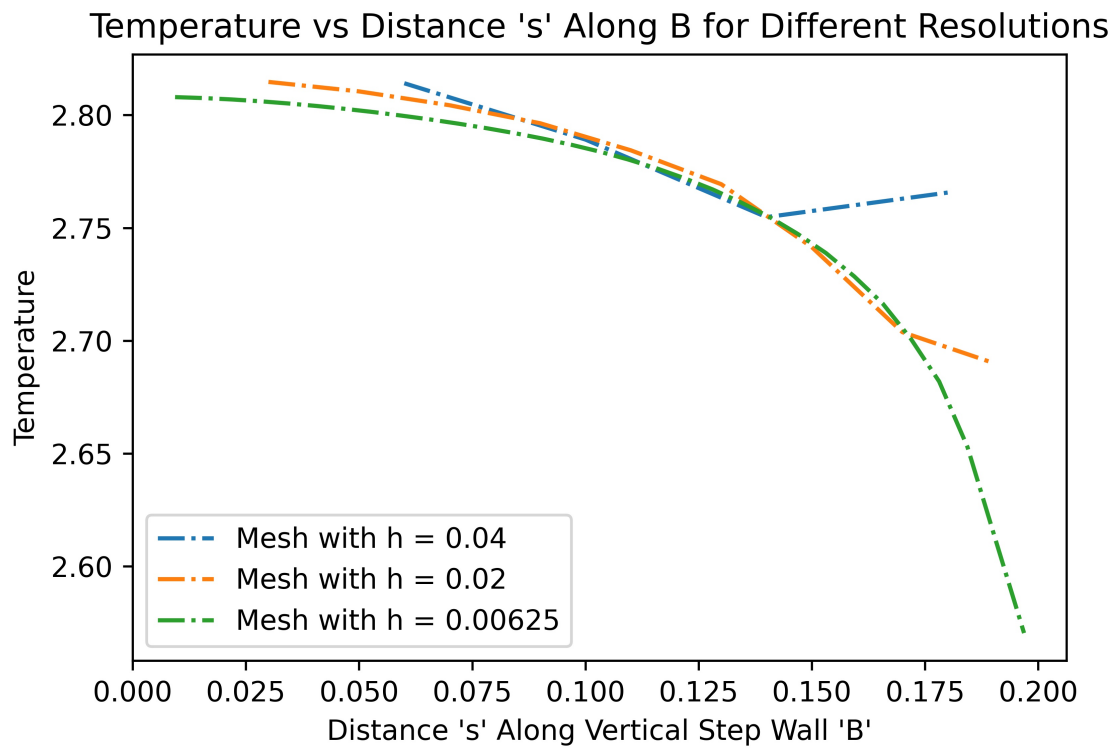




In referencing figures 1-3 for the pressure, density, and temperature fields across the bottom wall, "A", it is shown that the profiles are very similar, namely, the properties are approximately constant from the beginning of the wall to about 0.3 meters where they experience a sharp gradient as the flow moves across the normal shock wave boundary where theoretical behavior suggests that fluid density, pressure, and temperature increase rapidly across shock waves. These sharp gradients effectively confirm this expected behavior. Shortly after these sharp gradients (just removed from 0.3 meters from the beginning of the wall), the properties level off and nearly reach steady state. This behavior agrees with theory as the region downstream of the flow is isentropic (constant entropy) , and in this region, all thermodynamic properties are expected to remain relatively constant, or increase marginally with position. Furthermore, from all three plots we note that the solutions for the different spatial resolutions nearly overlap over [0,0.3 meters], and over [0.32,0.6 meters], while the largest differences in values are apparent over the normal shock wave region as expected. Additionally, in referencing the pressure plot, it is shown that the stagnation pressure approaches the theoretical value of approximately 12.06 Pa near the end of the bottom wall, where the simulation with the greatest refinement ( $h = 0.00625$ ) most closely approximates this expected value.

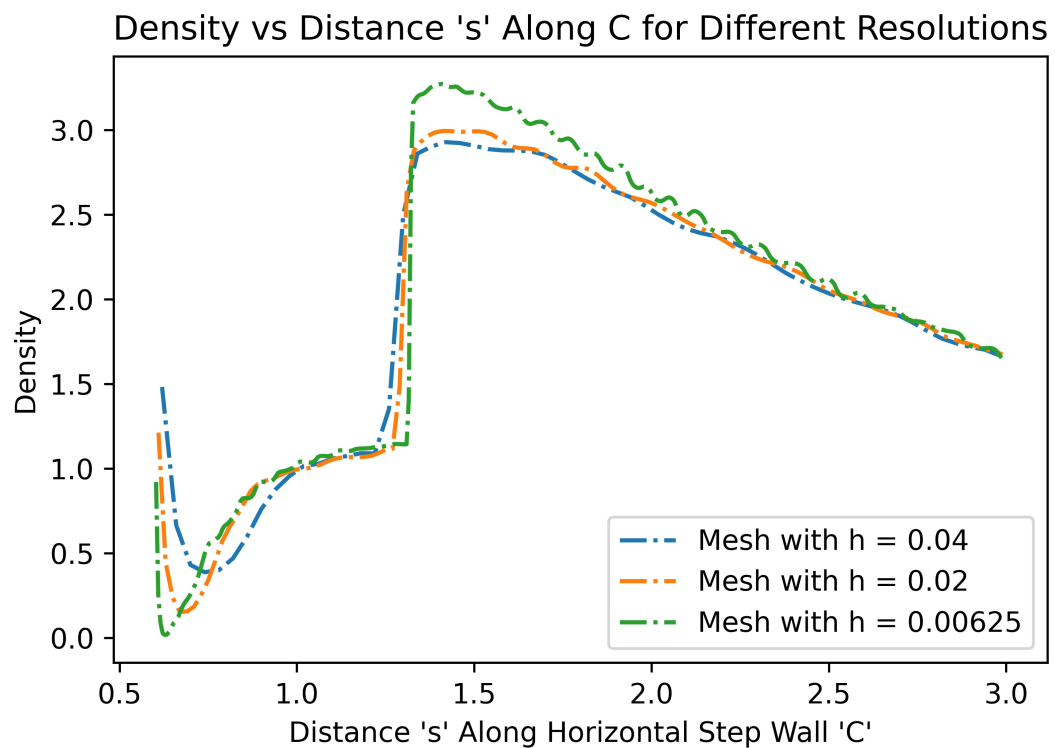
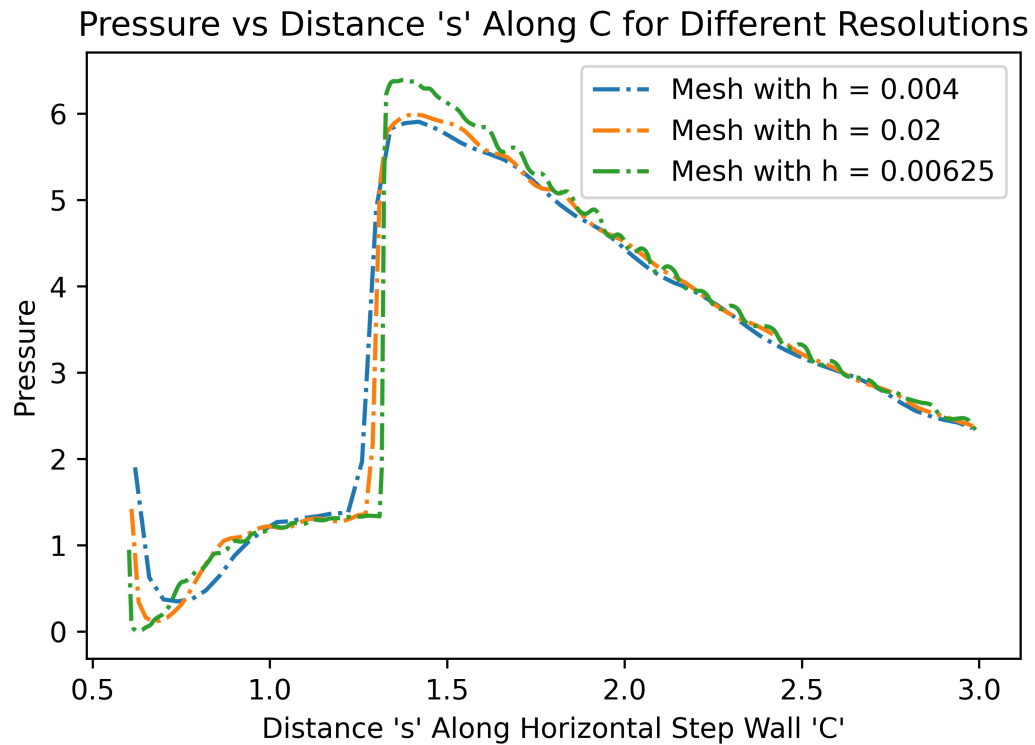
### Wall B Pressure, Density, Temperature:

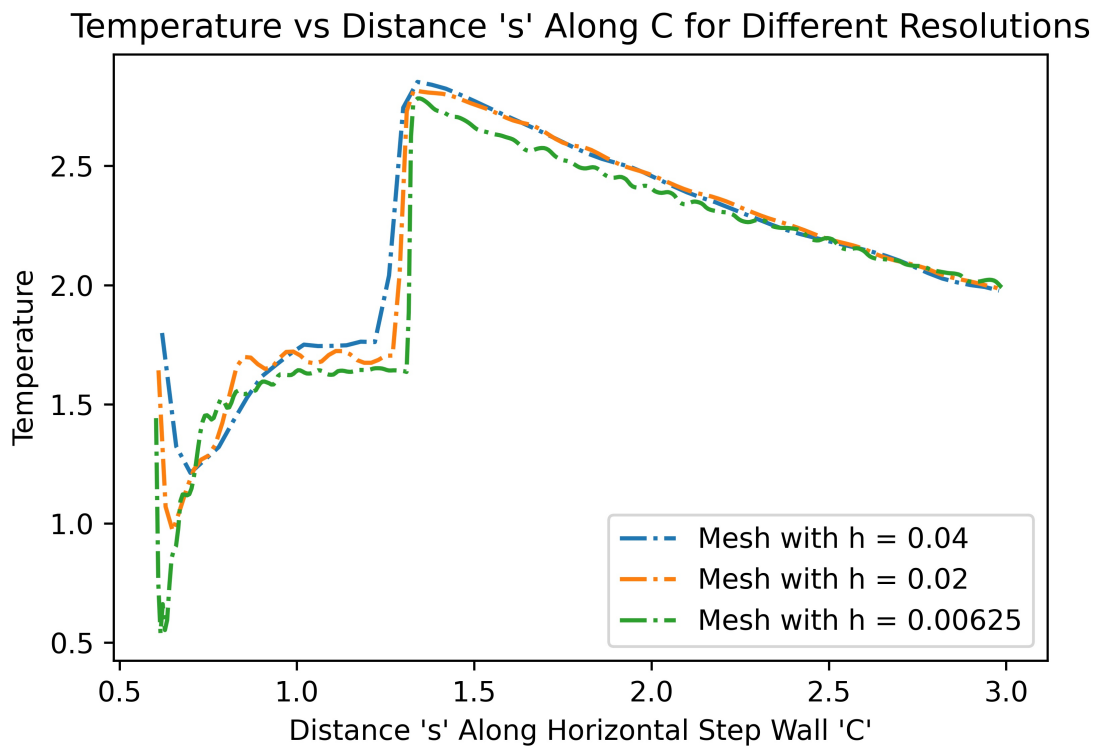




In referencing figures 4-6, the pressure, density, and temperature solutions all exhibit very similar behavior with position across the vertical step wall. In particular, the profiles are approximately inverted parabolic relationships where the properties decrease from a maximum value at the stagnation point to a minimum value at the top of the step wall where an expansion fan is realized.

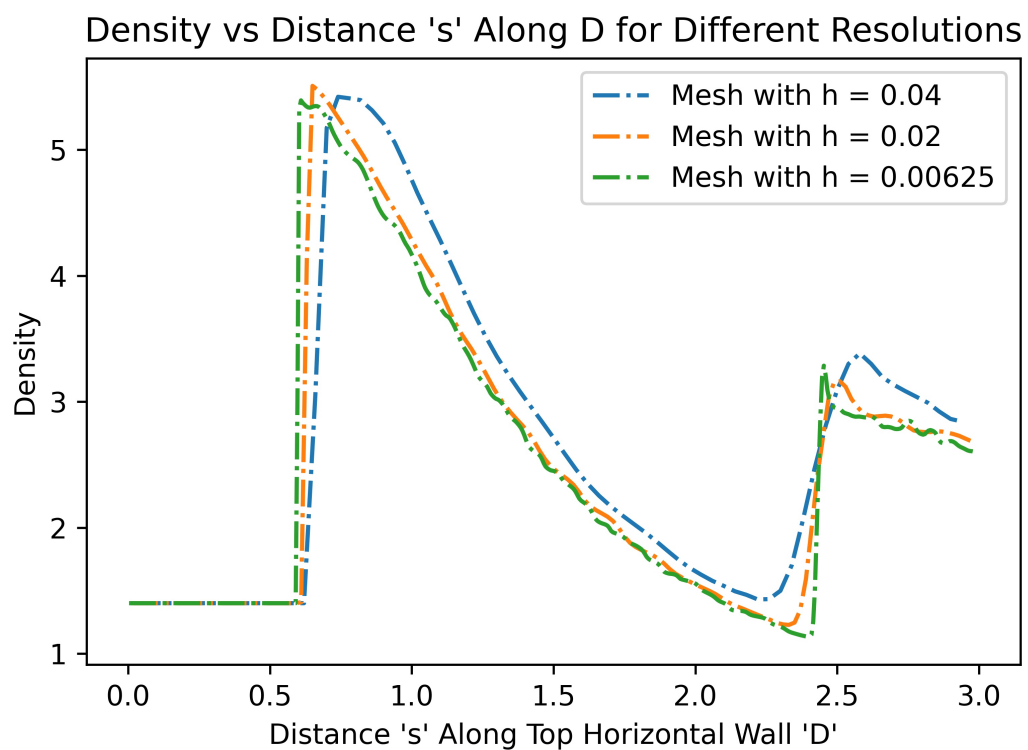
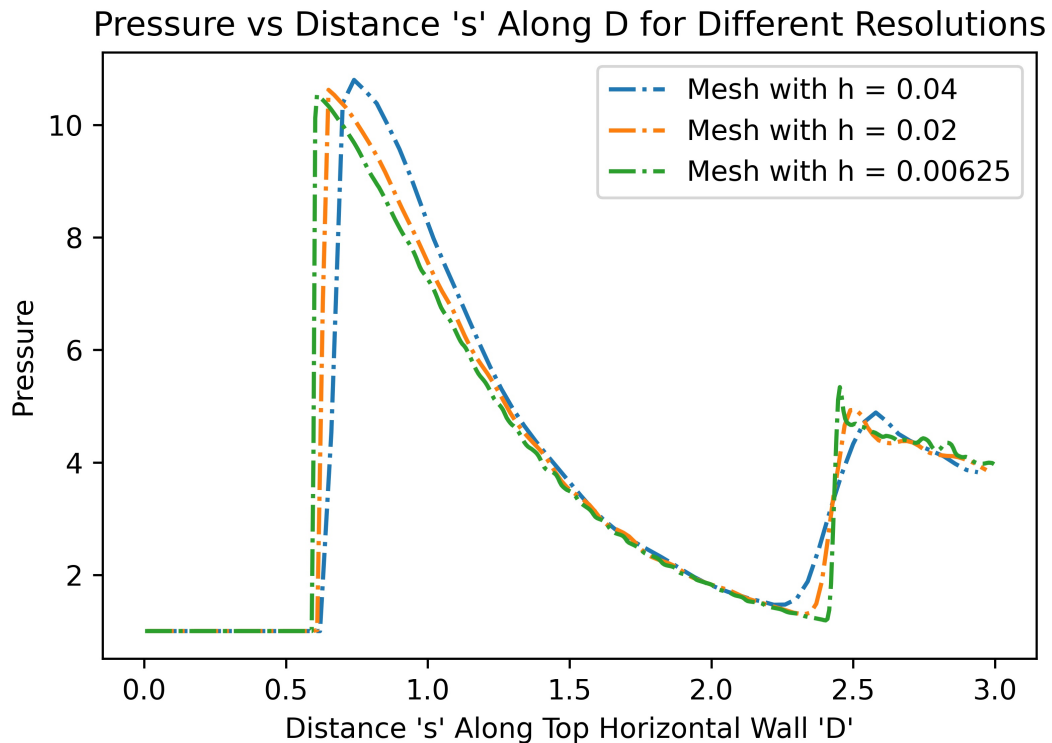
### Wall C Pressure, Density, Temperature:

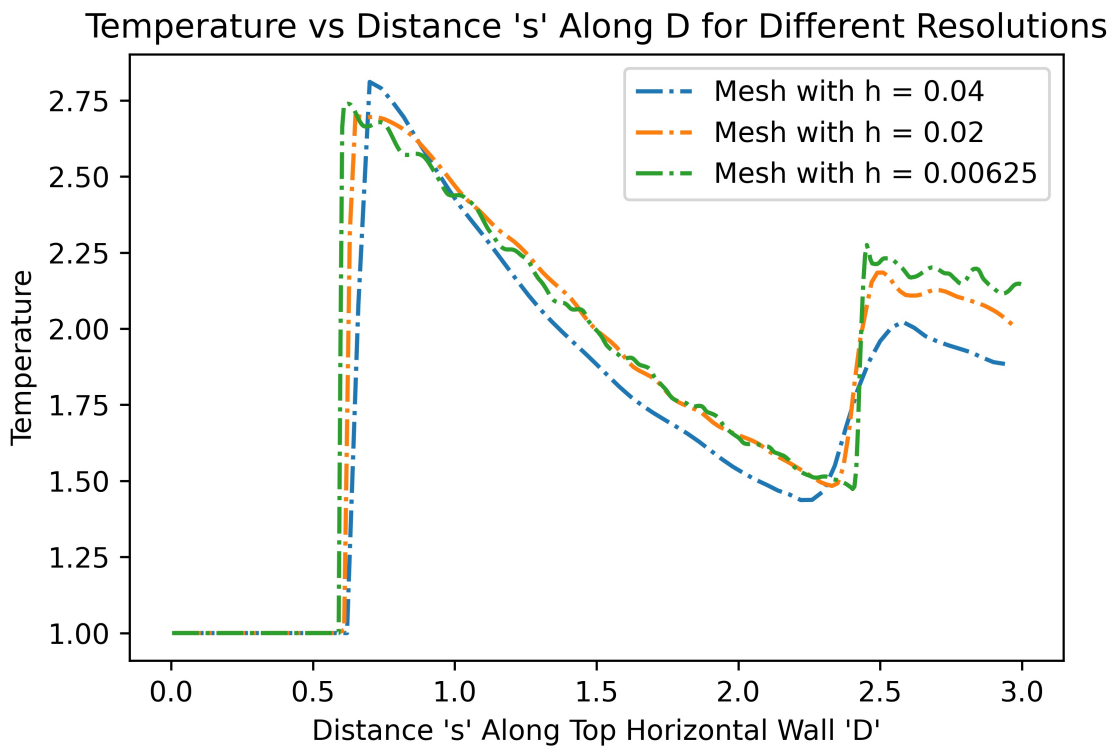




In referencing figures 7-9, it is again shown that the three solution fields exhibit similar properties with respect to position across the horizontal step wall. As expected, there is a large gradient at approximately 0.7 meters from the left end of the wall where the flow exhibits shock reflection at the intersection of two oblique shock waves.

#### Wall D Pressure, Density, Temperature:

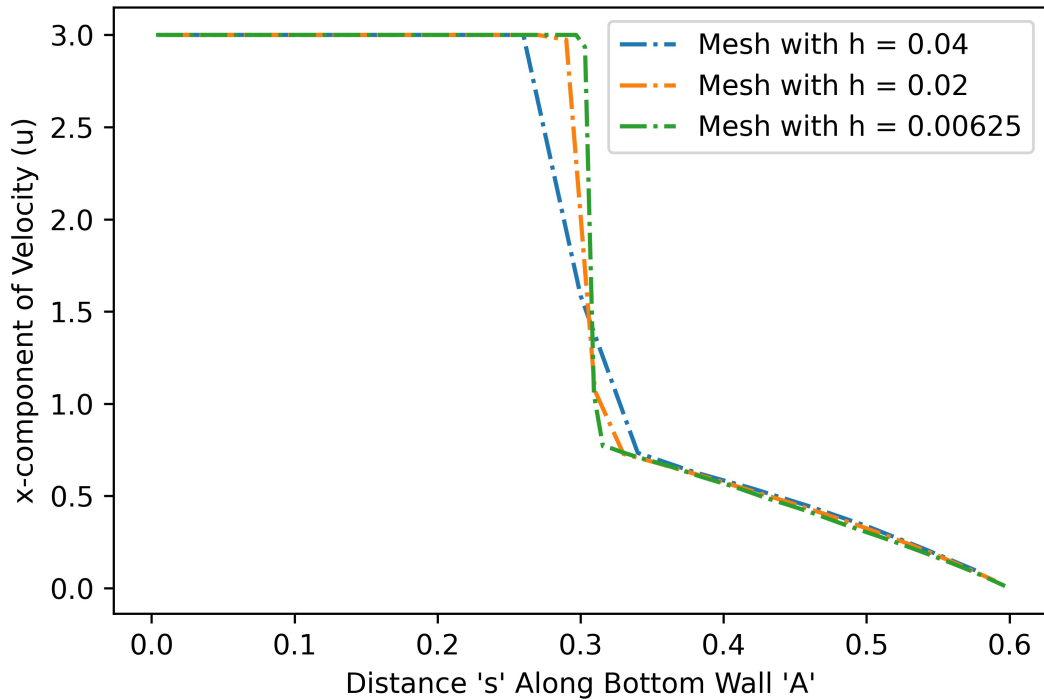




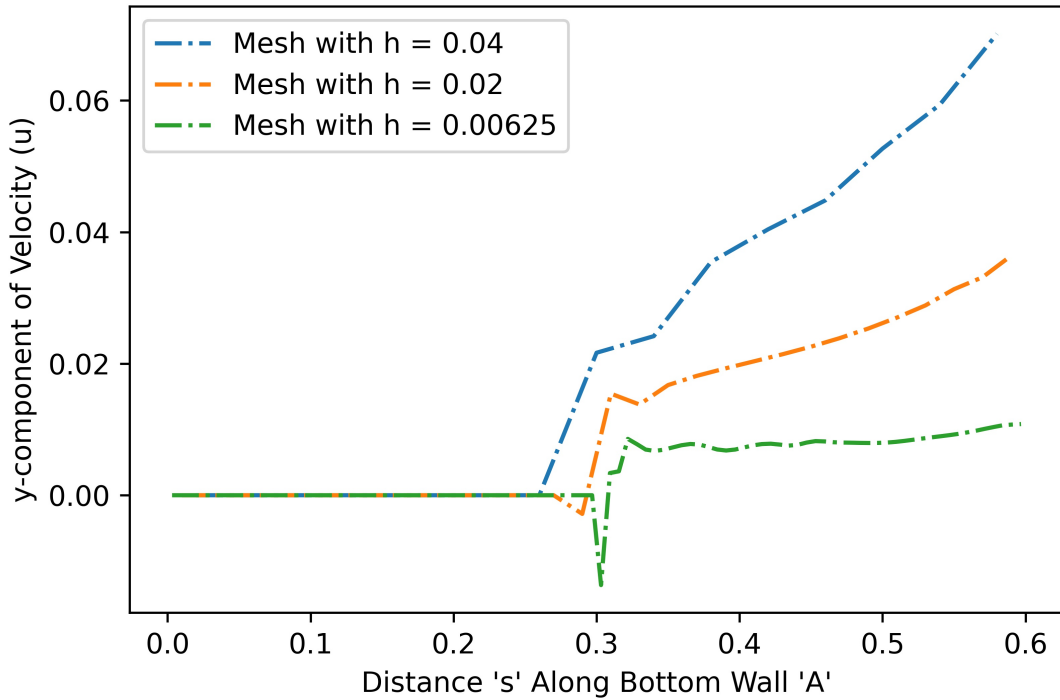
Shifting gears to figures 10-12, it is observed that the solution fields again remain relatively constant over 0.6 meters before increasing sharply where the flow exhibits its first shock reflection point. It then levels off between 0.7 meters and roughly 2.25 – 2.4 meters before experiencing a second sharp gradient as the flow encounters a second shock reflection point, before levelling off again. These behaviors thus agree with theoretical predictions.

#### **Velocity X and Y components along A,B,C,D :**

x-component of Velocity vs Distance Along A for Different Resolutions



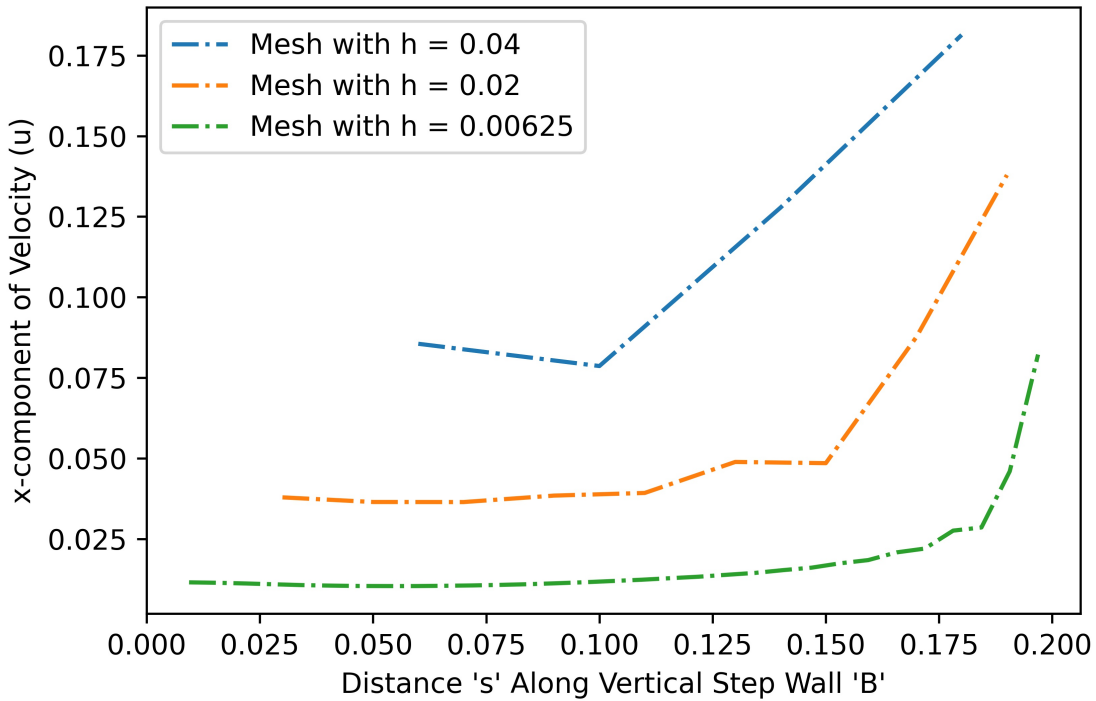
y-component of Velocity vs Distance Along A for Different Resolutions



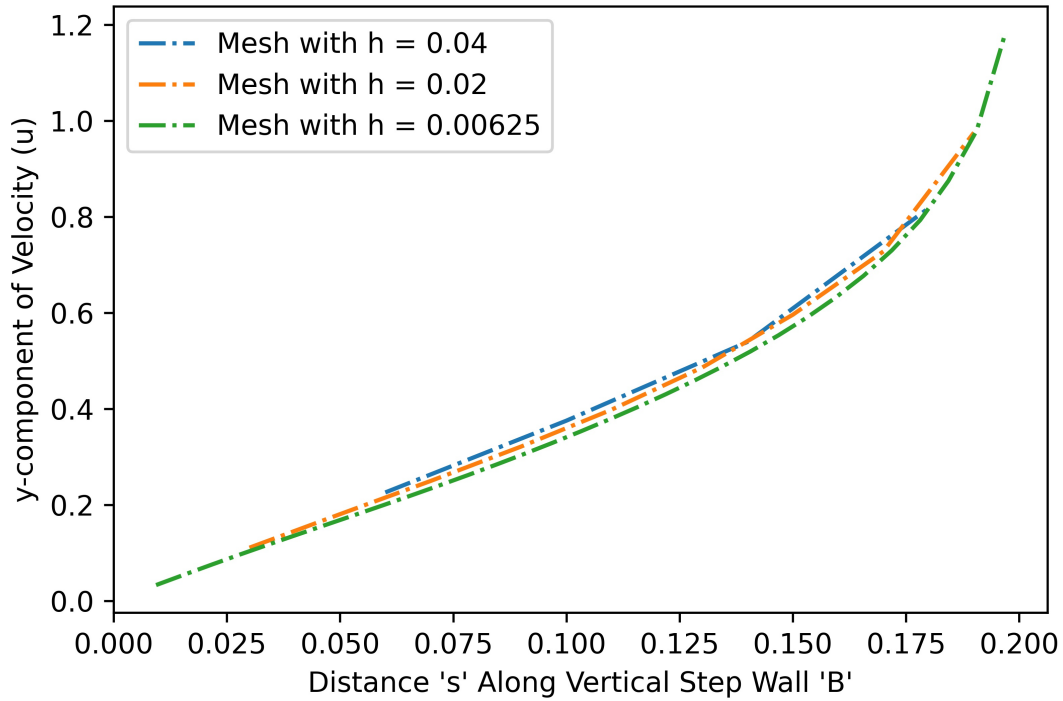
Transitioning now to the velocity field solutions, it is shown in figure 13 that the x-component of velocity remains constant before dropping off sharply at the shock wave where the Mach number decreases, and ultimately decreases linearly until the stagnation point. Figure 14 shows that the y-component of the velocity also begins at a constant value until reaching the shock wave where the

velocity increases somewhat sharply before exhibiting a linear relationship. Interestingly, the solution with the largest spatial resolution exhibits the steepest gradient from the shockwave onwards, while the one with the smallest resolution approximately levels out.

x-component of Velocity vs Distance Along B for Different Resolutions



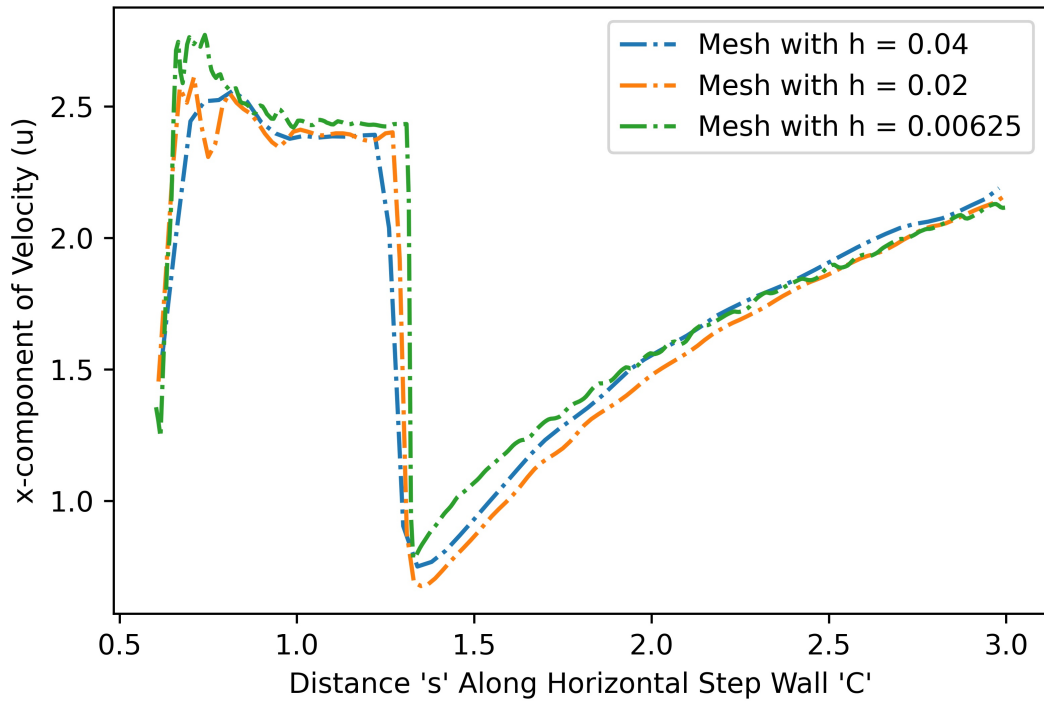
y-component of Velocity vs Distance Along B for Different Resolutions



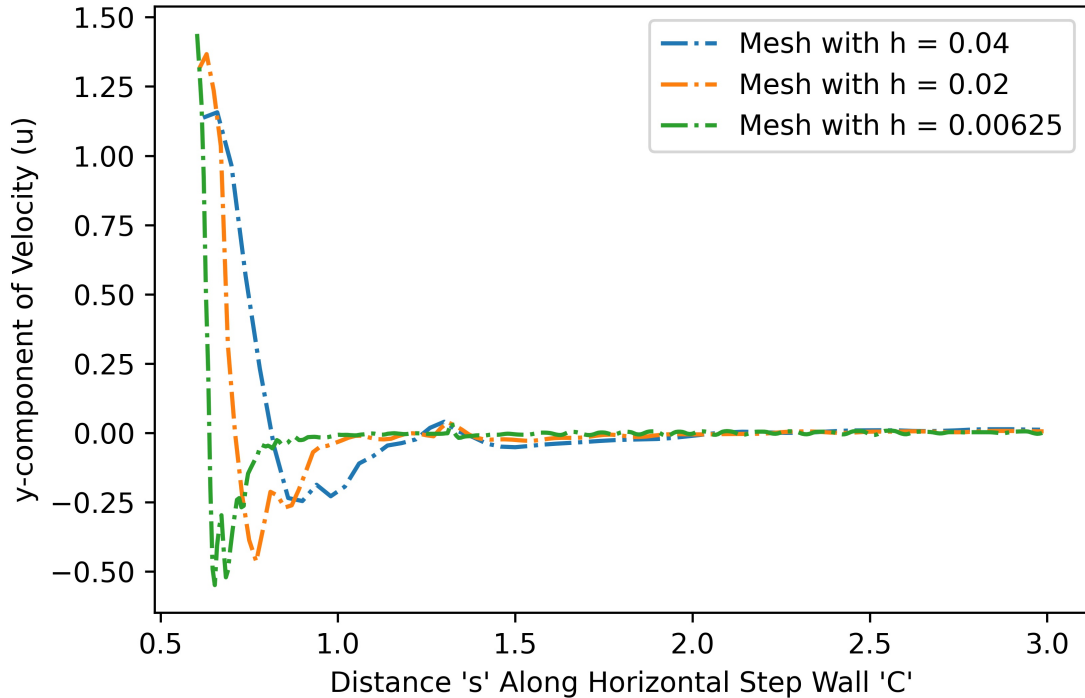
Looking at figure 15, it is shown that the x-component of velocity begins at a constant value before increasing roughly linearly. Interestingly, the spatial resolution greatly impacts the location where the velocity begins to increase. Conversely, figure 16 shows that the y-component of velocity

increases roughly parabolically with position, and there is nearly an overlap in the solutions for each of the resolutions. These behaviors are reasonable given that as position along the vertical step wall is increased, the flow moves further from the shock wave region (where the velocity is small given low Mach Number).

x-component of Velocity vs Distance Along C for Different Resolutions

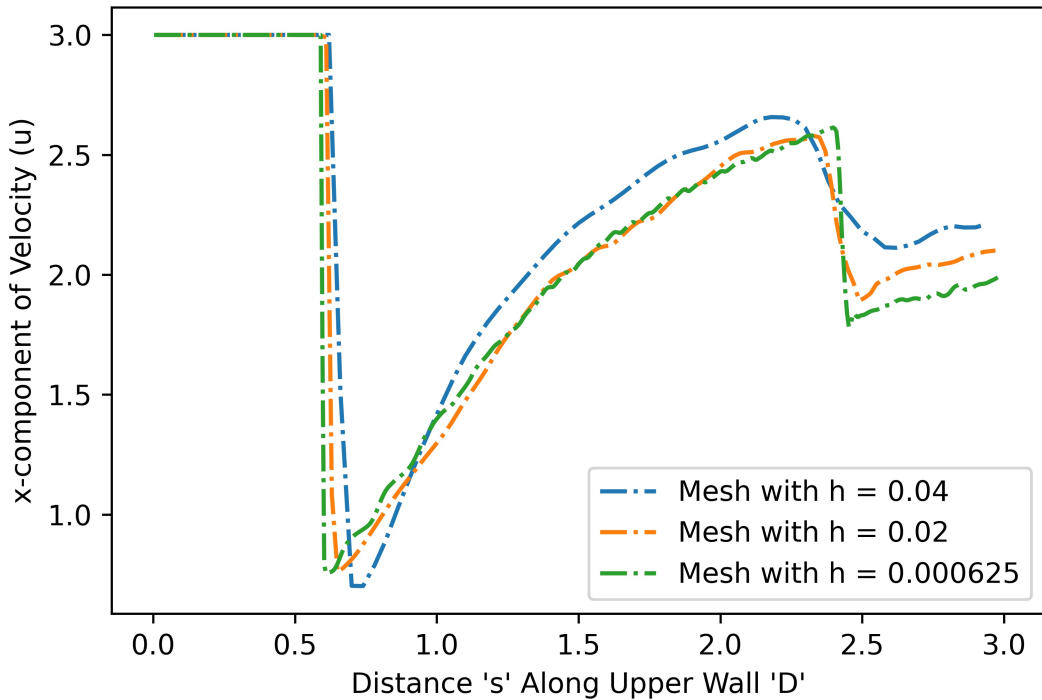


y-component of Velocity vs Distance Along C for Different Resolutions

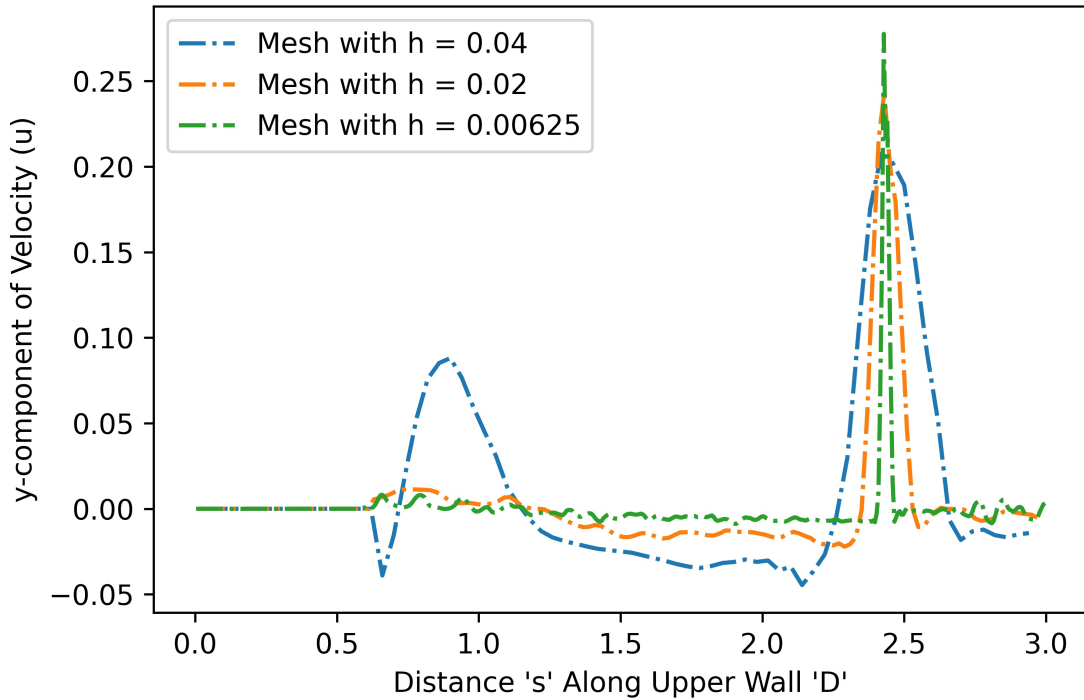


Looking now at figure 17, it is shown that the x-component of velocity increases rapidly at the beginning of the wall near the Mach Reflection region before levelling off, and then dropping sharply at the horizontal position corresponding to the first shock reflection point. It then increases from the first to the second shock reflection point. In referencing figure 18, it is shown that the y-component of velocity drops off significantly at the beginning of the wall before reaching negative values in what is likely a small recirculation region. It then levels off at approximately 0 around the first shock reflection point.

x-component of Velocity vs Distance Along D for Different Resolutions



y-component of Velocity vs Distance Along D for Different Resolutions



In transitioning to figure 19, it is observed that the x-component of velocity drops off sharply at the point at the shockwave along the upper wall before gradually increasing to a local maximum at the second shock reflection point, and then dropping off sharply. Lastly, in looking at figure 20, it is observed that the y-component of velocity is approximately zero over the entire upper wall until reaching the second shock reflection point.

### 5.10. Stagnation Pressure at Step

Note from the first two pressure plots, the pressure at the base of the step is slightly over 12Pa. The simulation measures a value of about 12.05Pa, which is in agreement with the theoretical calculation performed earlier.

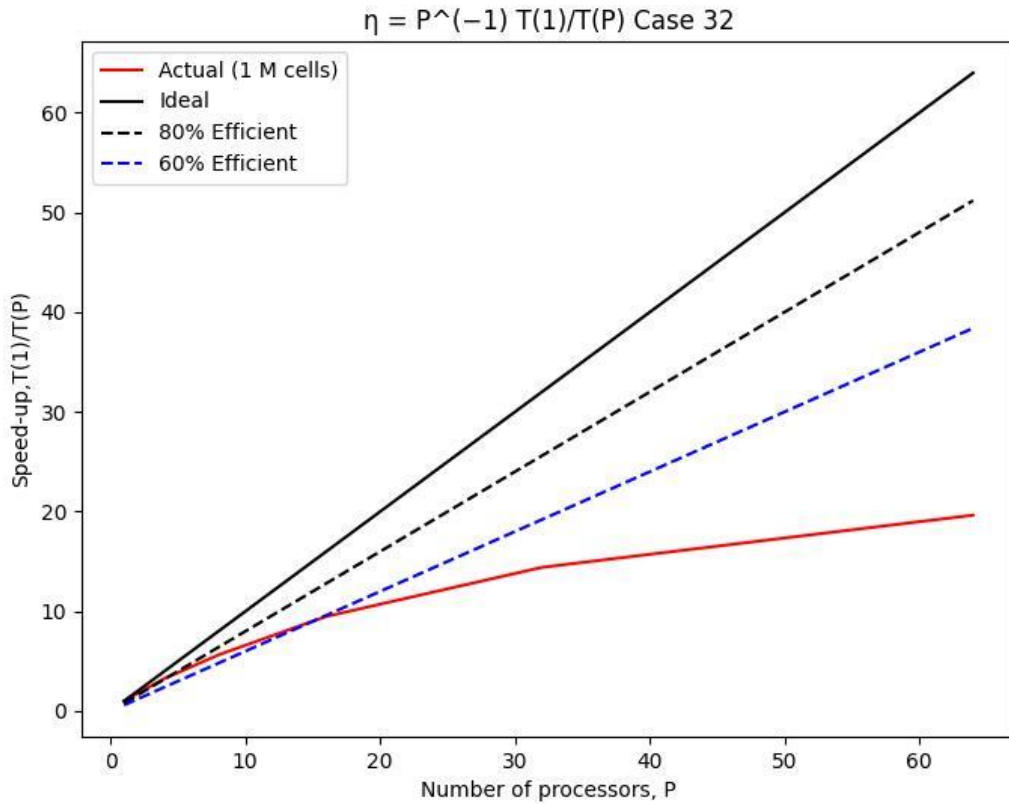
## 6. Parallel Performance Improvements

Define the speedup as the time taken for one processor ( $T(1)$ ) divided by the time taken for  $P$  processors ( $T(P)$ ). Similarly, let the parallel efficiency  $\eta$  be the speedup divided by  $P$ .

Note that the tables report the total  $T(P)$ , not that of single steps. The single step  $T(P)$  is used instead for the plots.

On a mesh of 64512 cells, for  $P$  ranging from 1 to 64 in steps of 2, the following scaling is obtained.

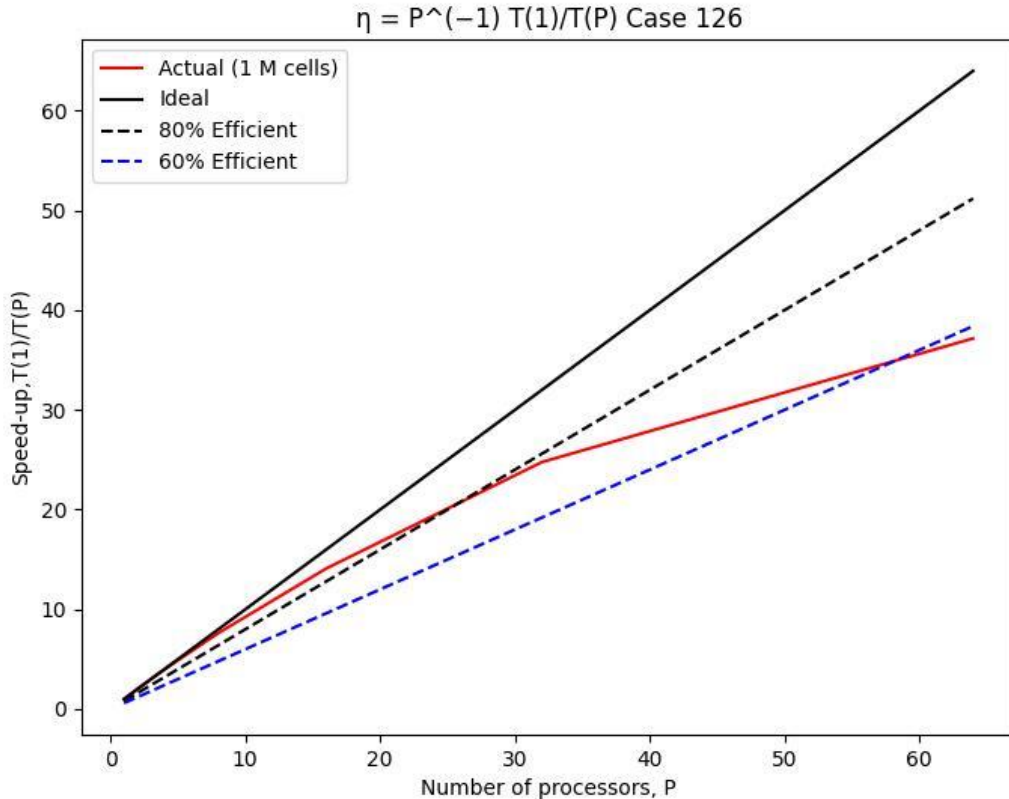
$T(P)$	Speedup $\eta$
4870.28	1.0000
2745.57	1.7738
1493.30	3.2614
0865.21	5.6290
0513.54	9.4837
0337.99	14.409
0247.94	19.642
	0.3069



A slightly improved scaling is obtained for a mesh of 1000188 cells.

$T(P)$  Speedup  $\eta$

270763.66	1.0000	1.0000
034192.10	2.0239	1.0119
034129.40	3.9783	0.9946
021542.00	14.094	0.8808
012256.70	24.765	0.7739
008170.29	37.171	0.5808



Clearly the larger mesh case scales much more nicely, which can be expected due to the more even load distribution.

## 7. References

- Allaire J, Xie Y, McPherson J, Luraschi J, Ushey K, Atkins A, Wickham H, Cheng J, Chang W, Iannone R (2021). *Rmarkdown: Dynamic Documents for r*. Retrieved from <https://CRAN.R-project.org/package=rmarkdown>
- Bengtsson H (2021). *R.utils: Various Programming Utilities*. Retrieved from <https://github.com/HenrikBengtsson/R.utils>
- Urbanek S (2021). *Jpeg: Read and Write JPEG Images*. Retrieved from <http://www.rforge.net/jpeg/>
- Xie Y (2013). “animation: An R Package for Creating Animations and Demonstrating Statistical Methods.” *Journal of Statistical Software*, **53**(1), 1–27. Retrieved from <https://doi.org/10.18637/jss.v053.i01>
- Xie Y (2014). “Knitr: A Comprehensive Tool for Reproducible Research in R.” In *Implementing reproducible computational research*, eds. V Stodden, F Leisch, and RD Peng,. Chapman; Hall/CRC. Retrieved from <http://www.crcpress.com/product/isbn/9781466561595>

- Xie Y (2015). *Dynamic Documents with R and Knitr* 2nd ed. Chapman; Hall/CRC, Boca Raton, Florida. Retrieved from <https://yihui.org/knitr/>
- Xie Y (2021a). *Animation: A Gallery of Animations in Statistics and Utilities to Create Animations*. Retrieved from <https://yihui.org/animation/>
- Xie Y (2021b). *Knitr: A General-Purpose Package for Dynamic Report Generation in r*. Retrieved from <https://yihui.org/knitr/>
- Xie Y, Allaire JJ, Grolemund G (2018). *R Markdown: The Definitive Guide*. Chapman; Hall/CRC, Boca Raton, Florida. Retrieved from <https://bookdown.org/yihui/rmarkdown>
- Xie Y, Dervieux C, Riederer E (2020). *R Markdown Cookbook*. Chapman; Hall/CRC, Boca Raton, Florida. Retrieved from <https://bookdown.org/yihui/rmarkdown-cookbook>

## 8. Appendix

Thank you so much for reading this work!

### Affiliation:

Justin Campbell  
Aerospace Department, University of Texas at Austin  
E-mail: [Campbelljustin989@gmail.com](mailto:Campbelljustin989@gmail.com) - jsc4348

### Affiliation:

Amanda Hiett  
Aerospace Department, University of Texas at Austin  
E-mail: [hiett.mandy@utexas.edu](mailto:hiett.mandy@utexas.edu) - amh7427

### Affiliation:

Akhil Sadam  
Aerospace Department, University of Texas at Austin  
E-mail: [akhil.sadam@utexas.edu](mailto:akhil.sadam@utexas.edu) - as97822